

**Supramolecular Assembly of Bent Dinuclear Amphiphilic Alkynylplatinum(II)
Terpyridine Complexes: Diverse Nanostructures Through Subtle Tuning of the Mode of
Molecular Stacking**

Sam Ka-Ming Leung, Alan Kwun-Wa Chan, Sammual Yu-Lut Leung, Ming-Yi Leung, and
Vivian Wing-Wah Yam*

Institute of Molecular Functional Materials (Areas of Excellence Scheme, University Grants Committee (Hong Kong)) and Department of Chemistry, The University of Hong Kong, Pokfulam Road (Hong Kong)

E-mail: wwyam@hku.hk

Electronic Supplementary Information (ESI)

Photophysical Measurements and Instrumentation

¹H NMR spectra were recorded on a Bruker AVANCE 400 (400 MHz) or a Bruker Ascend 500 (500 MHz) Fourier-transform NMR spectrometer with chemical shifts relative to tetramethylsilane (Me₄Si). Positive electron ionization (EI) mass spectra were recorded by using a Thermo Scientific DFS high-resolution magnetic sector mass spectrometer. Positive-ion electrospray ionization (ESI) mass spectra were recorded on a Bruker maXis II high-resolution ESI-QTOF mass spectrometer. The UV–visible absorption spectra were recorded on a Varian Cary 50 UV–visible spectrophotometer with the monitoring of temperature using the Varian Cary single-cell Peltier thermostat. The emission spectra were recorded on a Spex Fluorolog-3 model FL3-211 fluorescence spectrofluorometer equipped with an R2658P PMT detector. All solutions for the photophysical studies were degassed on a high-vacuum line in a two-compartment cell consisting of a 10 mL Pyrex bulb and a 1 cm-path length quartz cuvette and sealed from the atmosphere by a Bibby Rotaflo HP6 Teflon stopper. The solutions were rigorously degassed with at least four successive freeze–pump–thaw cycles. Transient absorption spectra were obtained using an Edinburgh Instrument LP980KS transient absorption spectrometer. Emission lifetimes were measured on Edinburgh Instrument LP980KS spectrometer. The excitation source is a Spectra-Physics Quanta-Ray Q-switched Lab-150 pulsed Nd:YAG laser (10 Hz) with a 355-nm output (third harmonic, 8 ns). The emission decay signals were captured by a Hamamatsu R928 PMT which was connected to a Tektronix Model TDS-3012C (100 MHz, 1.25 GS s⁻¹) digital oscilloscope and analyzed using the exponential fit (tail-fit data analysis) with the model $I(t) = I_0 \exp(-t/\tau)$, where $I(t)$ and I_0 stand for the luminescence intensities at times t and 0. Luminescence quantum yields in solution were measured by the optical dilute method described by Demas and Crosby¹ with a degassed aqueous solution of [Ru(bpy)₃]Cl₂ (excitation wavelength = 436 nm, Φ_{em} = 0.042) as reference and corrected for the refractive index of the solution.² Transmission electron microscopy (TEM)

experiments were conducted on a Philips Tecnai G2 20 S-TWIN or on a Philips CM100 Transmission Electron Microscope with an accelerating voltage of 200 kV. Pure carbon TEM grid, which does not have formvar layers, was employed in these studies in order to ensure the morphologies formed were solely due to the solutions themselves, not solvation of the formvar layer by dichloromethane. Scanning electron microscopy (SEM) experiments were conducted on a Hitachi S4800 FEG Scanning Electron Microscope. AFM topographical images and phase images were obtained using an Asylum MFP3D Atomic Force Microscope with an ARC2 SPM Controller under constant temperature and atmospheric pressure. The PXRD data were recorded on a Bruker AXS D8 ADVANCE (Philips PW1830) powder X-ray diffractometer in Bragg-Brentano ($\theta/2\theta$) reflection mode with a graphite monochromatized Cu–K α radiation ($\lambda = 1.54178 \text{ \AA}$) and nickel filter.

Temperature-dependent Nucleation–Elongation Model in Curve Fitting

Temperature-dependent nucleation–elongation model, developed by Meijer and co-workers,³ was applied to fit the experimental data in the variable-temperature UV–vis spectroscopic studies in DMSO solutions. All cooling curves obtained were performed at a slow cooling rate of 0.5 K min⁻¹ to ensure the self-assembly processes were under thermodynamic control.³

The nucleation regime and the elongation regime are governed by equations (1) and (2) respectively:

$$\phi_n = K_a^{1/3} \exp \left[(2/3 K_a^{-1/3} - 1) \frac{h_e}{RT_e^2} (T - T_e) \right] \quad (1)$$

$$\phi_n = \phi_{SAT} \left(1 - \exp \left[-\frac{h_e}{RT_e^2} (T - T_e) \right] \right) \quad (2)$$

where ϕ_n is the degree of aggregation, ϕ_{SAT} is a factor introduced to the equation such that ϕ_n/ϕ_{SAT} does not exceed unity, h_e is the molecular enthalpy released due to non-covalent interactions during elongation process, T_e is the elongation temperature, K_a is the dimensionless equilibrium constant of the nucleation process at T_e , and R is the universal gas constant.

The number-averaged degree of polymerization averaged over all active species in the elongation regime at a temperature T , $\langle N_n \rangle$, is given by equation (3):

$$\langle N_n(T) \rangle = \frac{1}{\sqrt{K_a}} \frac{\phi_n}{\phi_{SAT} - \phi_n} \quad (3)$$

The number-averaged degree of polymerization averaged over all active nucleated species at T_e is given by equation (4):

$$\langle N_n(T_e) \rangle = \frac{1}{\sqrt[3]{K_a}} \quad (4)$$

Solvent-dependent Nucleation–Elongation Equilibrium Model in Curve Fitting

In the nucleation–elongation model for solvent-dependent self-assembly, reported by Meijer and co-workers,⁴ the Gibbs free energy gain upon monomer addition, $\Delta G^\circ'$, is linearly correlated with the good solvent volume fraction f :

$$\Delta G^\circ' = \Delta G^\circ + m \cdot f$$

where ΔG° is the Gibbs free energy gain upon monomer addition in poor solvent and m is the parameter showing the dependence of $\Delta G^\circ'$ on f . The normalized degree of aggregation was deduced from the changes in UV–vis absorption band maxima:

$$\text{Normalized degree of aggregation} = \frac{\text{Abs}(f) - \text{Abs}(f=0)}{\text{Abs}(f=1) - \text{Abs}(f=0)}$$

The simulation and the curve-fitting with the equilibrium model were performed using Matlab R2013a under an isodesmic system.⁴

Crystal Structure Determination

The X-ray diffraction data of **9** were collected on a Bruker D8 VENTURE Dual source X-ray Diffractometer, using Mo K α radiation ($\lambda = 0.71073 \text{ \AA}$). The program SAINT V8.38A (Bruker AXS Inc., 2017) was used for the cell refinement and data reduction; XT, VERSION 2014/5 was used to solve the structure; SHELXL2018/3 (Sheldrick, 2018) was used to refine the structure.⁵ All e.s.d.'s (except the e.s.d. in the dihedral angle between two least-squares (l.s.) planes) are estimated using the full covariance matrix. The cell e.s.d.'s are taken into account individually in the estimation of e.s.d.'s in distances, angles and torsion angles; correlations between e.s.d.'s in cell parameters are only used when they are defined by crystal symmetry. An approximate (isotropic) treatment of cell e.s.d.'s is used for estimating e.s.d.'s involving l.s. planes. Table S1 summarizes the crystallographic and structural refinement data. Table S2 shows selected bond lengths and angles of **9**. CCDC 1945676 contains the crystallographic data of **9**. These data can be obtained free of charge from the Cambridge Crystallographic Data Centre via www.ccdc.cam.ac.uk/data_request/cif.

Computational Details

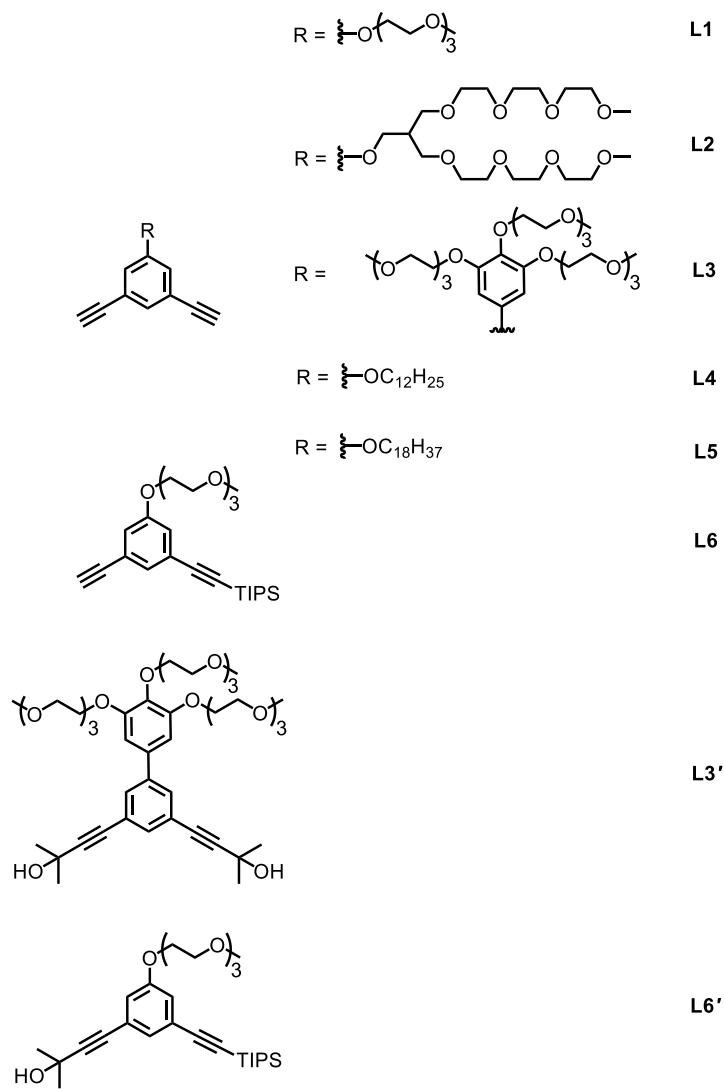
Calculations were performed using the Gaussian 09 software package.⁶ Density functional theory (DFT) with the M06 functional,⁷ which is recommended for studies of transition metal thermochemistry and for properly considering noncovalent interactions,^{7,8} was used to optimize the head-to-tail structure of the cationic model complex of **1**, in which the triethylene glycol substituent and all the octadecyloxy groups were replaced by methoxy groups, in conjunction with the solvation model density (SMD) continuum method⁹ using dichloromethane as the solvent. Vibrational frequencies were then calculated at the same level of theory for the optimized geometries to verify that each was a minimum (NIMAG = 0) on the potential energy surface. The Stuttgart effective core potentials (ECPs) and the associated basis set were used to describe platinum¹⁰ with two f-type polarization functions ($\zeta = 0.70$ and 0.14),¹¹ whereas the 6-31G(d,p) basis set was employed to describe all other atoms.^{12–15} All DFT calculations were performed with a pruned (99,590) grid for numerical integration. The Cartesian coordinates of the structures are shown in Tables S4–5.

Experimental Section

Materials and Reagents

[Pt{tpy-C₆H₄-(OC₁₈H₃₇)₂-3,5}Cl]OTf, [Pt{tpy-C₆H₄-(OC₄H₉)₂-3,5}Cl]OTf, [Pt{4',4'',4'''-tri-*tert*-butyl-tpy}Cl]OTf and [Pt{tpy-C₆H₄-(OTE₂)₂-3,5}Cl]OTf were synthesized according to previously reported literature.¹⁶ Potassium tetrachloroplatinate(II) (K₂[PtCl₄]) (Chem. Pur., 98 %), 2-methyl-3-butyn-2-ol (Fluorochem Ltd., 95 %), (triisopropylsilyl)acetylene (GFS Chemical Co. Ltd, 97 %), triethylamine (Fluorochem Ltd., 99 %), triethylene glycol monomethyl ether (Sigma-Aldrich, 95 %), 1-bromododecane (Alfa Aesar, 98 %), 1-bromoocadecane (Alfa Aesar, 98 %), 3,5-dibromophenol (Combi-Blocks Inc., 98 %), 1,3,5-tribromobenzene (Combi-Blocks Inc., 98 %), 5-bromo-1,2,3-trimethoxybenzene (Combi-Blocks Inc., 98 %), bis(pinacolato)diboron (Combi-Blocks Inc., 97 %), *p*-toluenesulfonyl chloride (J&K Scientific, 99 %) and boron tribromide (J&K Scientific, 1.0 M solution in CH₂Cl₂) were purchased from the corresponding chemical companies. Dimethyl sulfoxide (99+, for spectroscopy) was purchased from Sigma-Aldrich. All other reagents and solvents were of analytical grade and were used as received.

Synthesis and Characterization of the *meta*-Phenylene Ethynylene (*m*PE) Ligands



Scheme S1 Structures of the *meta*-phenylene ethynylene (*m*PE) ligands and their precursors.

All reactions were carried out under an inert atmosphere of nitrogen using standard Schlenk techniques. **L1**,¹⁷ **L2**,¹⁸ **L4**,¹⁹ **L5**,²⁰ **L3'**^{21–23} and **L6'**^{24–26} were synthesized according to previously reported literature.

Synthesis of L3. To a solution of **L3'** (1.02 g, 1.26 mmol) in degassed toluene was added NaOH (153 mg, 3.81 mmol). The solution was stirred for 1 hour at room temperature. The solvent was removed under reduced pressure and the crude product was purified by column chromatography on silica gel using dichloromethane–acetone (5:1, v/v) as the eluent to give

L3 as a yellow oil. Yield: 498 mg (57 %). ^1H NMR (400 MHz, CDCl_3 , 298 K, δ/ppm): $\delta = 3.12$ (s, 2H, $-\text{C}\equiv\text{CH}$), 3.37 (s, 6H, $-\text{OCH}_3$), 3.38 (s, 3H, $-\text{OCH}_3$), 3.51–3.57 (m, 6H, $-\text{OCH}_2-$), 3.62–3.69 (m, 12H, $-\text{OCH}_2-$), 3.71–3.77 (m, 6H, $-\text{OCH}_2-$), 3.82 (t, $J = 5.1$ Hz, 2H, $-\text{OCH}_2-$), 3.87 (t, $J = 5.1$ Hz, 4H, $-\text{OCH}_2-$), 4.19 (t, $J = 5.1$ Hz, 2H, $-\text{OCH}_2-$), 4.23 (t, $J = 5.1$ Hz, 4H, $-\text{OCH}_2-$), 6.77 (s, 2H, phenyl), 7.56 (t, $J = 1.6$ Hz, 1H, phenyl), 7.61 (d, $J = 1.6$ Hz, 2H, phenyl). Positive-ion HR-EI MS: calcd for $\text{C}_{37}\text{H}_{52}\text{O}_{12}$ m/z 688.3459; found m/z 688.3453 [M] $^+$.

Synthesis of L6. The procedure was similar to that for **L3**, except **L6'** (570 mg, 1.13 mmol) was used in place of **L3'**. The crude product was purified by column chromatography on silica gel using dichloromethane as the eluent to give **L6** as a yellow oil. Yield: 300 mg (60 %). ^1H NMR (400 MHz, CDCl_3 , 298 K, δ/ppm): $\delta = 1.12$ (m, 21H, $-\text{Si}\{\text{CH}(\text{CH}_3)_2\}_3$), 3.05 (s, 1H, $-\text{C}\equiv\text{CH}$), 3.38 (s, 3H, $-\text{OCH}_3$), 3.53–3.58 (m, 2H, $-\text{OCH}_2-$), 3.63–3.70 (m, 4H, $-\text{OCH}_2-$), 3.70–3.76 (m, 2H, $-\text{OCH}_2-$), 3.84 (t, $J = 4.8$ Hz, 2H, $-\text{OCH}_2-$), 4.12 (t, $J = 4.8$ Hz, 2H, $-\text{OCH}_2-$), 6.99 (m, 2H, phenyl), 7.20 (t, $J = 1.5$ Hz, 1H, phenyl). Positive-ion HR-EI MS: calcd for $\text{C}_{26}\text{H}_{40}\text{O}_4\text{Si}$ m/z 444.2696; found m/z 444.2684 [M] $^+$.

Synthesis and Characterization of the Mono- and Dinuclear Alkynylplatinum(II) Terpyridine Complexes with the *mPE* Ligands

Synthesis of 1. To a solution of **L1** (45 mg, 0.16 mmol) and [Pt{tpy-C₆H₄-(OC₁₈H₃₇)₂-3,5}Cl]OTf (476 mg, 0.39 mmol) in degassed dichloromethane (30 mL) containing triethylamine (5 mL) was added a catalytic amount of CuI. The solution was stirred overnight at room temperature. The solvent was removed under reduced pressure and the crude product was purified by column chromatography on silica gel using dichloromethane-methanol (10:1, v/v) as the eluent. Recrystallization through a slow diffusion of diethyl ether vapor into a concentrated dichloromethane solution of **1** afforded an orange solid. Yield: 220 mg (53 %). ¹H NMR (400 MHz, DMSO-d₆, 353 K, δ/ppm): δ = 0.86 (t, J = 6.8 Hz, 12H, -CH₃), 1.26 (m, 112H, -CH₂-), 1.50 (t, J = 6.8 Hz, 8H, -CH₂-), 1.80 (t, J = 6.8 Hz, 8H, -CH₂-), 3.28 (s, 3H, -OCH₃), 3.45–3.69 (m, 8H, -OCH₂-), 3.82 (t, J = 4.7 Hz, 2H, -OCH₂-), 4.16 (t, J = 6.8 Hz, 8H, -OCH₂-), 4.22 (t, J = 4.7 Hz, 2H, -OCH₂-), 6.79 (t, J = 2.1 Hz, 2H, phenyl), 7.03 (s, 2H, phenyl), 7.29 (m, 5H, phenyl), 8.00 (td, J = 6.4 Hz, J = 1.3 Hz, 4H, tpy), 8.54 (td, J = 7.9 Hz, J = 1.3 Hz, 4H, tpy), 8.91 (d, J = 7.9 Hz, 4H, tpy), 8.96 (s, 4H, tpy), 9.31 (d, J = 6.4 Hz, 4H, tpy). Positive-ion HR-ESI MS: calcd for [C₁₃₁H₁₉₂N₆O₈Pt₂]²⁺ *m/z* 1184.2056; found *m/z* 1184.2043 [M-2OTf]²⁺.

Synthesis of 2. The procedure was similar to that for **1**, except [Pt{tpy-C₆H₄-(OC₄H₉)₂-3,5}Cl]OTf (383 mg, 0.39 mmol) was used in place of [Pt{tpy-C₆H₄-(OC₁₈H₃₇)₂-3,5}Cl]OTf. Recrystallization through a slow diffusion of diethyl ether vapor into a concentrated dichloromethane solution of **2** afforded an orange solid. Yield: 162 mg (54 %). ¹H NMR (500 MHz, DMSO-d₆, 353 K, δ/ppm): δ = 1.00 (t, J = 6.8 Hz, 12H, -CH₃), 1.53 (m, 8H, -CH₂-), 1.79 (m, 8H, -CH₂-), 3.27 (s, 3H, -OCH₃), 3.45–3.69 (m, 8H, -OCH₂-), 3.83 (t, J = 4.6 Hz, 2H, -OCH₂-), 4.16 (t, J = 6.8 Hz, 8H, -OCH₂-), 4.22 (t, J = 4.6 Hz, 2H, -OCH₂-), 6.79 (t, J = 2.0 Hz, 2H, phenyl), 7.00 (s, 2H, phenyl), 7.27 (s, 1H,

phenyl), 7.30 (d, J = 2.0 Hz, 4H, phenyl), 7.98 (t, J = 6.8 Hz, 4H, tpy), 8.53 (t, J = 8.0 Hz, 4H, tpy), 8.93 (d, J = 8.0 Hz, 4H, tpy), 8.96 (s, 4H, tpy), 9.28 (d, J = 6.8 Hz, 4H, tpy). Positive-ion HR-ESI MS: calcd for $[C_{75}H_{80}N_6O_8Pt_2]^{2+}$ m/z 791.2661; found m/z 791.2609 $[M-2OTf]^{2+}$.

Synthesis of 3. The procedure was similar to that for **1**, except **L2** (110 mg, 0.16 mmol) was used in place of **L1**. Recrystallization through a slow diffusion of diethyl ether vapor into a concentrated dichloromethane solution of **3** afforded an orange solid. Yield: 273 mg (59 %).

1H NMR (500 MHz, DMSO-*d*₆, 353 K, δ /ppm): δ = 0.86 (t, J = 6.8 Hz, 12H, -CH₃), 1.25 (m, 112H, -CH₂-), 1.49 (m, 8H, -CH₂-), 1.79 (m, 8H, -CH₂-), 2.32 (m, 1H, -CH(OCH₂)₂-), 3.20 (d, J = 5.3 Hz, 4H, -OCH₂-), 3.23 (s, 6H, -OCH₃), 3.40–3.62 (m, 24H, -OCH₂-), 4.11 (d, J = 5.3 Hz, 2H, -OCH₂-), 4.15 (t, J = 6.8 Hz, 8H, -OCH₂-), 6.78 (t, J = 1.5 Hz, 2H, phenyl), 7.00 (d, J = 1.5 Hz, 2H, phenyl), 7.27 (t, J = 1.5 Hz, 1H, phenyl), 7.29 (d, J = 1.5 Hz, 4H, phenyl), 7.99 (td, J = 5.7 Hz, J = 1.4 Hz, 4H, tpy), 8.55 (td, J = 7.9 Hz, J = 1.4 Hz, 4H, tpy), 8.91 (d, J = 7.9 Hz, 4H, tpy), 8.96 (s, 4H, tpy), 9.30 (d, J = 5.7 Hz, 4H, tpy). Positive-ion HR-ESI MS: calcd for $[C_{142}H_{214}N_6O_{13}Pt_2]^{2+}$ m/z 1301.2791; found m/z 1301.2737 $[M-2OTf]^{2+}$.

Synthesis of 4. The procedure was similar to that for **1**, except **L3** (110 mg, 0.16 mmol) was used in place of **L1**. The crude product was purified by column chromatography on silica gel using dichloromethane-methanol (8:1, v/v) as the eluent. Recrystallization through a slow diffusion of diethyl ether vapor into a concentrated dichloromethane solution of **4** afforded an orange solid. Yield: 220 mg (45 %). 1H NMR (400 MHz, DMSO-*d*₆, 353 K, δ /ppm): δ = 0.86 (t, J = 6.7 Hz, 12H, -CH₃), 1.26 (m, 112H, -CH₂-), 1.50 (t, J = 6.7 Hz, 8H, -CH₂-), 1.80 (t, J = 6.7 Hz, 8H, -CH₂-), 3.24 (s, 6H, -OCH₃), 3.28 (s, 3H, -OCH₃), 3.42–3.68 (m, 18H, -OCH₂-), 3.76 (t, J = 4.6 Hz, 6H, -OCH₂-), 3.83 (t, J = 4.6 Hz, 6H, -OCH₂-), 4.16 (t, J = 6.7 Hz, 8H, -OCH₂-), 4.29 (t, J = 4.6 Hz, 6H, -OCH₂-), 6.79 (t, J = 2.0 Hz, 2H, phenyl), 7.02 (s, 2H, phenyl), 7.30 (d, J = 2.0 Hz, 4H, phenyl), 7.65 (s, 1H, phenyl), 7.66 (s, 2H, phenyl), 8.00 (td, J = 6.0 Hz, J = 1.6 Hz, 4H, tpy), 8.56 (td, J = 8.1 Hz, J = 1.6 Hz, 4H, tpy), 8.92 (d,

J = 8.1 Hz, 4H, tpy), 8.97 (s, 4H, tpy), 9.35 (d, *J* = 6.0 Hz, 4H, tpy). Positive-ion HR-ESI MS: calcd for [C₁₅₁H₂₂₄N₆O₁₆Pt₂]²⁺ *m/z* 1384.3106; found *m/z* 1384.3058 [M–2OTf]²⁺.

Synthesis of 5. The procedure was similar to that for **1**, except [Pt{tpy–C₆H₄–(OTE_G)₂-3,5}Cl]OTf (695 mg, 0.69 mmol) was used in place of [Pt{tpy–C₆H₄–(OC₁₈H₃₇)₂-3,5}Cl]OTf, and **L4** (85 mg, 0.27 mmol) was used in place of **L1**. Recrystallization through a slow diffusion of diethyl ether vapor into a concentrated dichloromethane solution of **5** afforded a red solid. Yield: 372 mg (60 %). ¹H NMR (400 MHz, DMSO-*d*₆, 353 K, δ/ ppm): δ = 0.85 (t, *J* = 6.7 Hz, 3H, –CH₃), 1.16–1.81 (m, 20H, –CH₂–), 3.26 (s, 12H, –OCH₃), 3.44–3.48 (m, 8H, –OCH₂–), 3.53–3.62 (m, 16H, –OCH₂–), 3.62–3.70 (m, 8H, –OCH₂–), 3.84 (t, *J* = 4.8 Hz, 8H, –OCH₂–), 4.08 (t, *J* = 6.7 Hz, 2H, –OCH₂–), 4.30 (t, *J* = 4.8 Hz, 8H, –OCH₂–), 6.85 (t, *J* = 1.5 Hz, 2H, phenyl), 6.99 (d, *J* = 1.5 Hz, 2H, phenyl), 7.26 (d, *J* = 1.5 Hz, 1H, phenyl), 7.35 (d, *J* = 1.5 Hz, 4H, phenyl), 7.98 (td, *J* = 6.0 Hz, *J* = 1.3 Hz, 4H, tpy), 8.54 (td, *J* = 7.9 Hz, *J* = 1.3 Hz, 4H, tpy), 8.90 (d, *J* = 7.9 Hz, 4H, tpy), 8.97 (s, 4H, tpy), 9.29 (d, *J* = 6.0 Hz, 4H, tpy). Positive-ion HR-ESI MS: calcd for [C₉₂H₁₁₄N₆O₁₇Pt₂]²⁺ *m/z* 982.8773; found *m/z* 982.8733 [M–2OTf]²⁺.

Synthesis of 6. The procedure was similar to that for **1**, except [Pt{tpy–C₆H₄–(OTE_G)₂-3,5}Cl]OTf (695 mg, 0.69 mmol) was used in place of [Pt{tpy–C₆H₄–(OC₁₈H₃₇)₂-3,5}Cl]OTf, and **L5** (63 mg, 0.16 mmol) was used in place of **L1**. Recrystallization through a slow diffusion of diethyl ether vapor into a concentrated dichloromethane solution of **6** afforded a red solid. Yield: 221 mg (59 %). ¹H NMR (400 MHz, DMSO-*d*₆, 353 K, δ/ ppm): δ = 0.85 (t, *J* = 6.8 Hz, 3H, –CH₃), 1.19–1.44 (m, 28H, –CH₂–), 1.50 (t, *J* = 6.8 Hz, 2H, –CH₂–), 1.78 (t, *J* = 6.8 Hz, 2H, –CH₂–), 3.27 (s, 12H, –OCH₃), 3.42–3.51 (m, 8H, –OCH₂–), 3.52–3.63 (m, 16H, –OCH₂–), 3.63–3.71 (m, 8H, –OCH₂–), 3.85 (t, *J* = 4.7 Hz, 8H, –OCH₂–), 4.08 (t, *J* = 6.8 Hz, 2H, –OCH₂–), 4.31 (t, *J* = 4.7 Hz, 8H, –OCH₂–), 6.84 (t, *J* = 1.6 Hz, 2H, phenyl), 6.95 (d, *J* = 1.6 Hz, 2H, phenyl), 7.22 (d, *J* = 1.6 Hz, 1H,

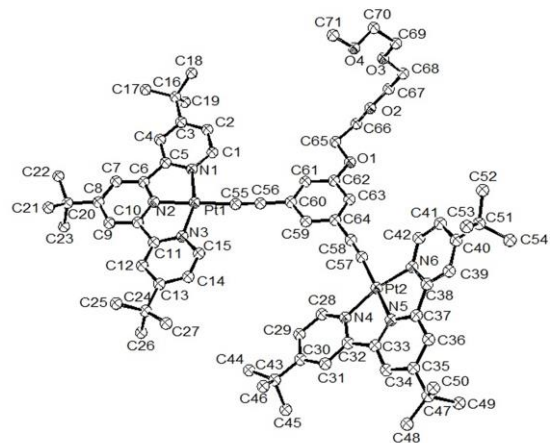
phenyl), 7.35 (d, J = 1.6 Hz, 4H, phenyl), 7.95 (td, J = 6.0 Hz, J = 1.5 Hz, 4H, tpy), 8.50 (td, J = 7.9 Hz, J = 1.5 Hz, 4H, tpy), 8.93 (d, J = 7.9 Hz, 4H, tpy), 8.97 (s, 4H, tpy), 9.26 (d, J = 6.0 Hz, 4H, tpy). Positive-ion HR-ESI MS: calcd for $[C_{98}H_{126}N_6O_{17}Pt_2]^{2+}$ m/z 1024.9243; found m/z 1024.9204 $[M-2OTf]^{2+}$.

Synthesis of 7. The procedure was similar to that for **1**, except $[Pt\{tpy-C_6H_4-(OTE\bar{G})_2-3,5\}Cl]OTf$ (695 mg, 0.69 mmol) was used in place of $[Pt\{tpy-C_6H_4-(OC_{18}H_{37})_2-3,5\}Cl]OTf$. Recrystallization through a slow diffusion of diethyl ether vapor into a concentrated dichloromethane solution of **7** afforded a red solid. Yield: 204 mg (57 %). 1H NMR (400 MHz, DMSO- d_6 , 353 K, δ /ppm): δ = 3.26 (s, 12H, $-OCH_3$), 3.27 (s, 3H, $-OCH_3$), 3.45–3.49 (m, 10H, $-OCH_2-$), 3.55–3.67 (m, 30H, $-OCH_2-$), 3.84 (t, J = 4.8 Hz, 10H, $-OCH_2-$), 4.22 (t, J = 4.8 Hz, 2H, $-OCH_2-$), 4.30 (t, J = 4.8 Hz, 8H, $-OCH_2-$), 6.85 (t, J = 2.0 Hz, 2H, phenyl), 6.99 (s, 2H, phenyl), 7.25 (s, 1H, phenyl), 7.35 (d, J = 2.0 Hz, 4H, phenyl), 7.96 (t, J = 6.6 Hz, 4H, tpy), 8.51 (t, J = 7.9 Hz, 4H, tpy), 8.92 (d, J = 7.9 Hz, 4H, tpy), 8.98 (s, 4H, tpy), 9.26 (d, J = 6.6 Hz, 4H, tpy). Positive-ion HR-ESI MS: calcd for $[C_{87}H_{104}N_6O_{20}Pt_2]^{2+}$ m/z 971.8305; found m/z 971.8301 $[M-2OTf]^{2+}$.

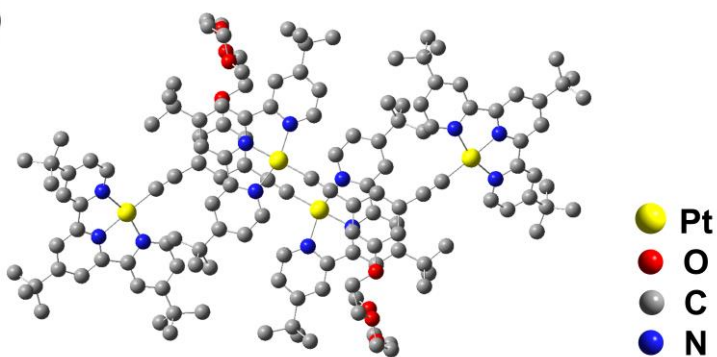
Synthesis of 8. The procedure was similar to that for **1**, except **L6** (218 mg, 0.49 mmol) was used in place of **L1**. Recrystallization through a slow diffusion of diethyl ether vapor into a concentrated dichloromethane solution of **8** afforded an orange solid. Yield: 267 mg (40 %). 1H NMR (400 MHz, CDCl₃, 298 K, δ /ppm): δ = 0.87 (t, J = 6.6 Hz, 6H, $-CH_3$), 1.15 (s, 21H, $-Si\{CH(CH_3)_2\}_3$), 1.20–1.52 (m, 64H, $-CH_2-$), 3.39 (s, 3H, $-OCH_3$), 3.55–3.60 (m, 2H, $-OCH_2-$), 3.65–3.80 (m, 6H, $-OCH_2-$), 3.90 (m, 6H, $-OCH_2-$), 4.18 (t, J = 4.9 Hz, 2H, $-OCH_2-$), 6.24 (s, 1H, phenyl), 6.82 (m, 3H, phenyl), 6.96 (s, 1H, phenyl), 7.06 (s, 1H, phenyl), 7.66 (t, J = 6.7 Hz, 2H, tpy), 8.39 (t, J = 8.1 Hz, 2H, tpy), 8.48 (s, 2H, tpy), 8.88 (d, J = 8.1 Hz, 2H, tpy), 9.23 (d, J = 6.7 Hz, 2H, tpy). Positive-ion HR-ESI MS: calcd for $[C_{83}H_{126}N_3O_6PtSi]^+$ m/z 1484.9081; found m/z 1484.9077 $[M-OTf]^+$.

Synthesis of 9. The procedure was similar to that for **1**, except [Pt{4',4'',4'''-tri-*tert*-butyl-tpy}Cl]OTf (305 mg, 0.39 mmol) was used in place of [Pt{tpy-C₆H₄-(OC₁₈H₃₇)₂-3,5}Cl]OTf. The crude product was purified by column chromatography on silica gel using dichloromethane-acetone (10:1, v/v) as the eluent. Recrystallization through a slow diffusion of diethyl ether vapor into a concentrated dichloromethane solution of **9** afforded yellow crystals suitable for X-ray analysis. Yield: 142 mg (50 %). ¹H NMR (400 MHz, CDCl₃, 298 K, δ/ ppm): δ = 1.42 (s, 36H, -CH₃), 1.51 (s, 18H, -CH₃), 3.40 (s, 3H, -OCH₃), 3.58–3.81 (m, 8H, -OCH₂-), 3.90 (t, J = 4.5 Hz, 2H, -OCH₂-), 4.21 (t, J = 4.5 Hz, 2H, -OCH₂-), 6.95 (s, 2H, phenyl), 7.54 (dd, J = 6.0 Hz, J = 1.7 Hz, 4H, tpy), 7.64 (s, 1H, phenyl), 8.34 (d, J = 1.7 Hz, 4H, tpy), 8.42 (s, 4H, tpy), 9.12 (d, J = 6.0 Hz, 4H, tpy). Positive-ion HR-ESI MS: calcd for [C₇₁H₈₈N₆O₄Pt₂]²⁺ m/z 739.3076; found m/z 739.3051 [M-2OTf]²⁺.

(a)



(b)



(c)

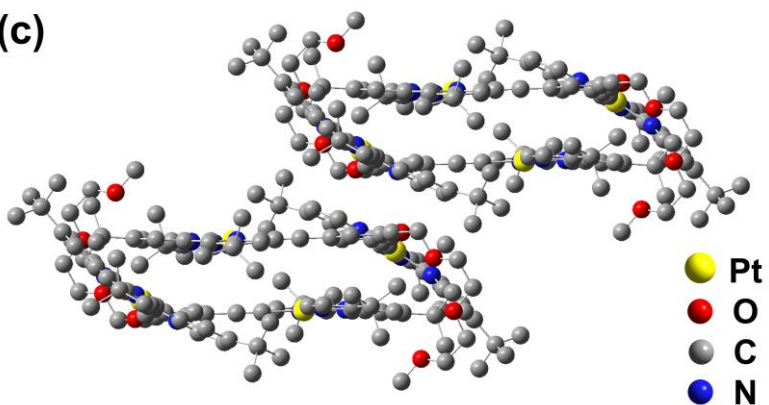


Fig. S1 (a) Perspective view of **9** with an atomic numbering scheme. The thermal ellipsoids are drawn at 50 % probability level. Hydrogen atoms, counter ions and solvent molecules are omitted for clarity. (b) Crystal packing diagram of **9** which shows the head-to-tail configuration. (c) Crystal packing diagram of **9** from the side view.

Table S1 Crystal and structure determination data of **9**.

Empirical formula	C ₇₇ H ₈₈ N ₆ O ₄ Pt ₂ ·2(CF ₃ O ₃ S)·3(CH ₂ Cl ₂)
Formula weight	2032.57
Temperature, K	173
Wavelength, Å	Mo <i>K</i> α, λ = 0.71073
Crystal system	Triclinic
Space group	<i>P</i> ī
<i>a</i> , Å	13.4362 (6)
<i>b</i> , Å	18.3994 (8)
<i>c</i> , Å	20.2998 (8)
α, °	106.666 (1)
β, °	108.577 (1)
γ, °	103.771 (1)
Volume, Å ³	4246.8 (3)
<i>Z</i> , Å ³	2
Density (calculated), g cm ⁻³	1.589
Crystal size	0.21 mm × 0.08 mm × 0.06 mm
Index ranges	$-16 \leq h \leq 16$ $-23 \leq k \leq 21$ $-23 \leq l \leq 25$
Reflections collected/unique	42364/17273
<i>GoF</i> on <i>F</i> ²	1.07
Final <i>R</i> indices [<i>I</i> > 2 σ(<i>I</i>)]	<i>R</i> ₁ = 0.057 <i>wR</i> ₂ = 0.133
Largest diff. peak and hole, e Å ⁻³	2.61 and -2.08

Table S2 Selected bond lengths and angles of **9** with estimated standard deviations (e.s.d.s.) in parentheses.

Bond	Length [Å]	Bonds	Angle [°]
Pt1–N1	2.027(6)	N2–Pt1–N1	80.8(3)
Pt1–N2	1.961(6)	N2–Pt1–N3	79.7(3)
Pt1–N3	2.025(7)	C55–Pt1–N1	98.5(3)
Pt1–C55	1.982(9)	C55–Pt1–N3	101.0(3)
Pt2–N4	2.007(7)	N3–Pt1–N1	160.5(3)
Pt2–N5	1.968(6)	N2–Pt1–C55	178.0(3)
Pt2–N6	2.011(7)	C56–C55–Pt1	175.9(8)
Pt2–C57	1.982(8)	N5–Pt2–N4	81.2(3)
Pt1…Pt1	4.931	N5–Pt2–N6	81.1(3)
Pt2…Pt2	4.615	C57–Pt2–N6	100.1(4)
		C57–Pt2–N4	97.6(3)
		N4–Pt2–N6	162.0(3)
		N5–Pt2–C57	178.5(3)
		C58–C57–Pt2	174.7(8)

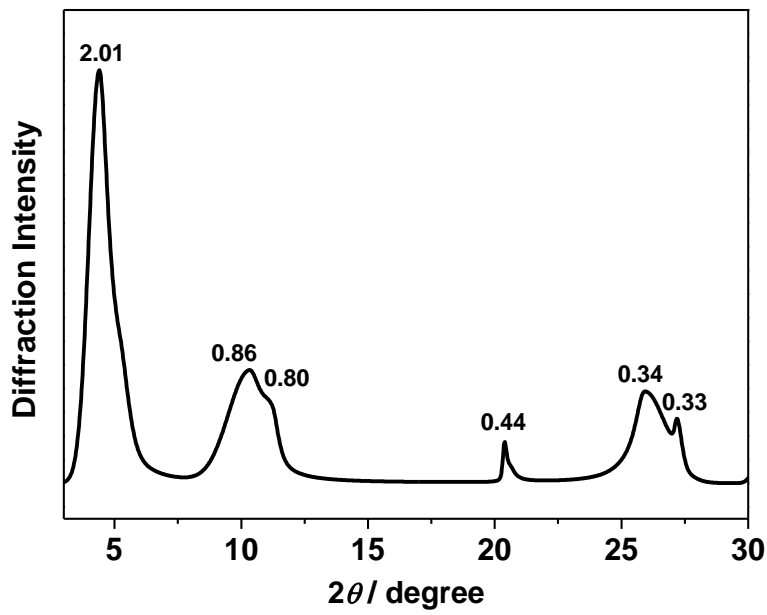


Fig. S2 PXRD pattern on the bulk sample of **6**. Numerical values indicate d -spacings (in nm).

Table S3 Photophysical data of **1–9** in dichloromethane at 298 K.

Complex	λ_{abs} [nm] ($\varepsilon/\text{dm}^3 \text{ mol}^{-1} \text{ cm}^{-1}$)	λ_{em} [nm] (τ_0 [μs])	$\Phi_{\text{lum}}^{\text{a}}$
1	339 (33840), 420 (13120), 475 (11810)	620 (0.47)	0.003
2	337 (27190), 420 (10030), 489 (7250)	628 (0.92)	0.030
3	319 (28690), 338 (29190), 419 (10950), 485 (7480)	632 (0.77)	0.026
4	345 (33450), 433 (16670), 480 (14740)	— ^b	— ^b
5	319 (33360), 341 (28010), 490 (14360)	642 (0.49)	0.004
6	342 (20550), 417 (7420), 484 (8850)	636 (0.52)	0.005
7	341 (18940), 421 (7050), 486 (8220)	637 (0.55)	0.005
8	344 (21250), 431 (8730), 479 (7100)	625 (0.97)	0.034
9	314 (25600), 341 (20260), 411 (6660), 466 (6330)	609 (1.31)	0.099

^a Relative luminescence quantum yield (Φ_{lum}) measured at room temperature using aqueous $[\text{Ru}(\text{bpy})_3]\text{Cl}_2$ solution as the reference (excitation wavelength = 436 nm, $\Phi_{\text{lum}} = 0.042$). ^b Non-emissive.

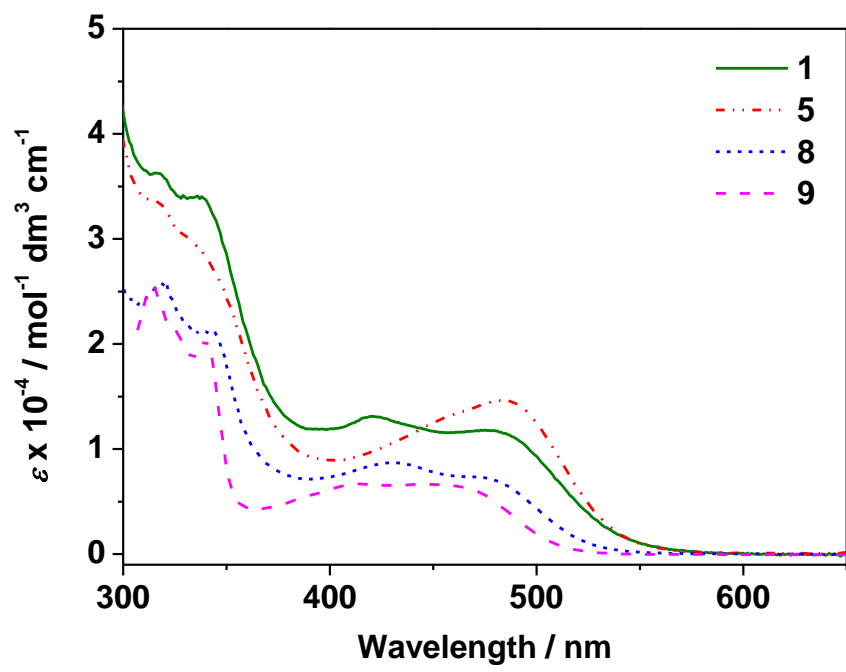


Fig. S3 Electronic absorption spectra of **1**, **5**, **8** and **9** in dichloromethane.

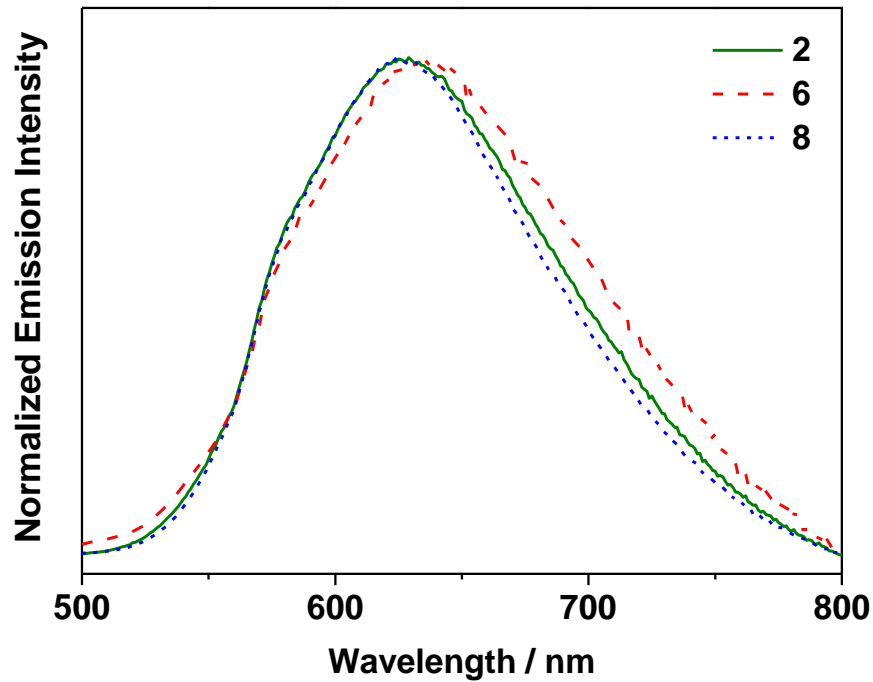


Fig. S4 Normalized emission spectra of **2**, **6** and **8** in degassed dichloromethane at 298 K.

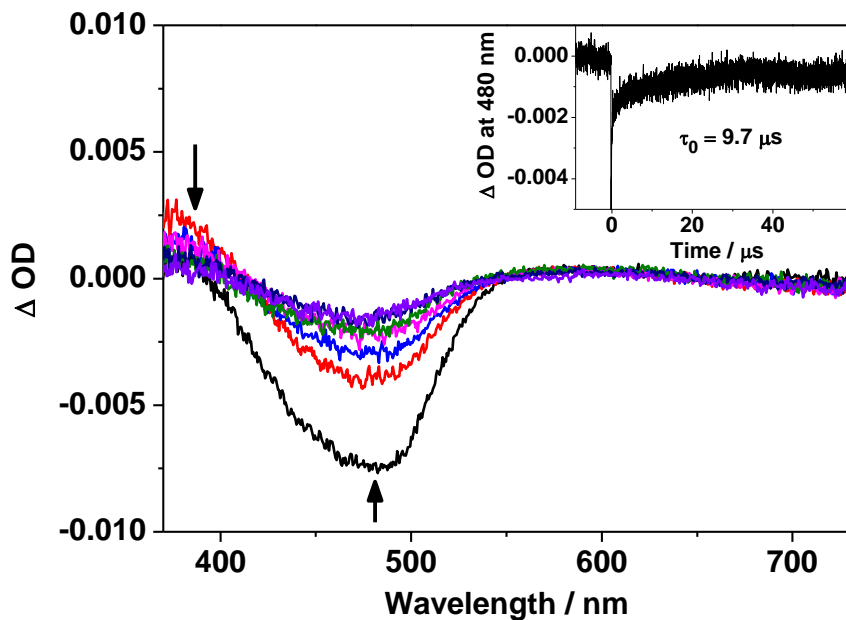


Fig. S5 Transient absorption difference spectra of **1** measured in dichloromethane at 298 K at decay times of 0 – 60 μs (at intervals of 10 μs) following a 355 nm laser pulse excitation. Inset: The decay trace of the absorption at 480 nm.

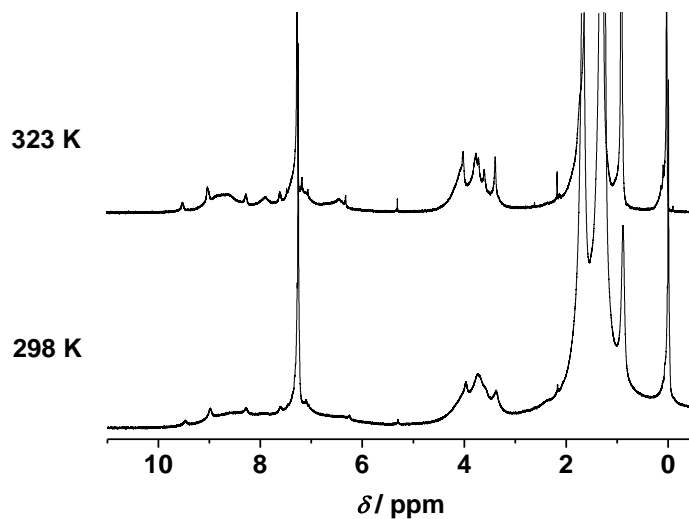


Fig. S6 ^1H NMR spectra of **1** in CDCl_3 at 298 and 323 K. ($[\text{Pt}] = 2.8 \times 10^{-3} \text{ M}$)

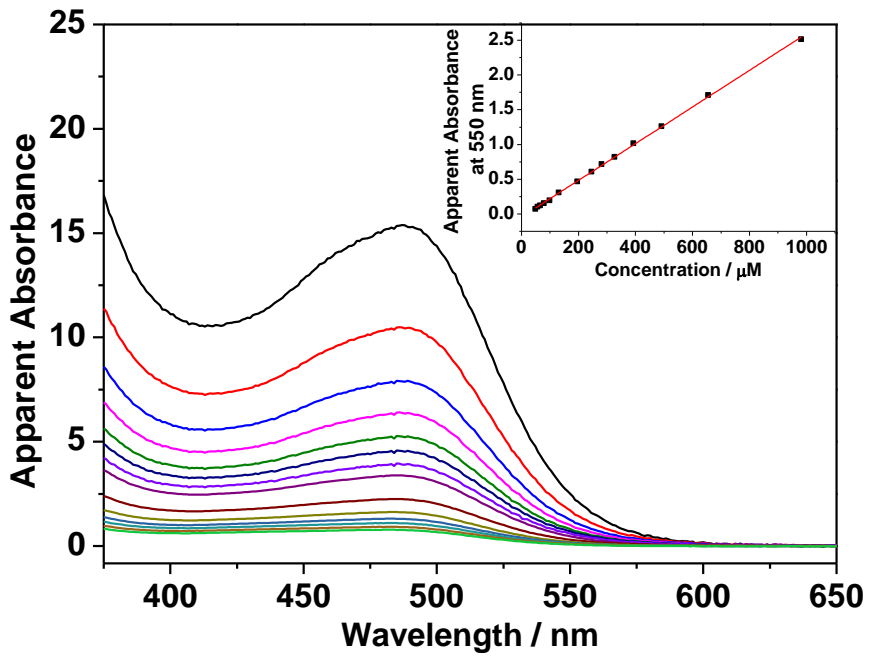


Fig. S7 UV–Vis absorption spectra of **1** in dichloromethane at various concentrations (4.9×10^{-5} – 9.8×10^{-4} M). Inset: A plot of absorbance at 550 nm against concentration. The apparent absorbance values have been obtained by correcting to a 1-cm path length equivalence.

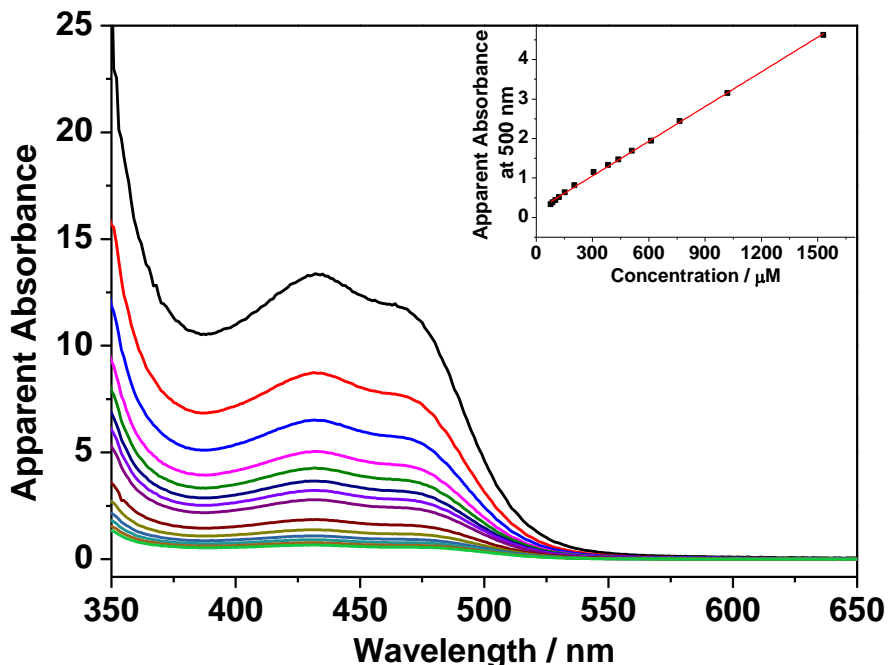


Fig. S8 UV–Vis absorption spectra of **8** in dichloromethane at various concentrations (7.7×10^{-5} – 1.5×10^{-3} M). Inset: A plot of absorbance at 500 nm against concentration. The apparent absorbance values have been obtained by correcting to a 1-cm path length equivalence.

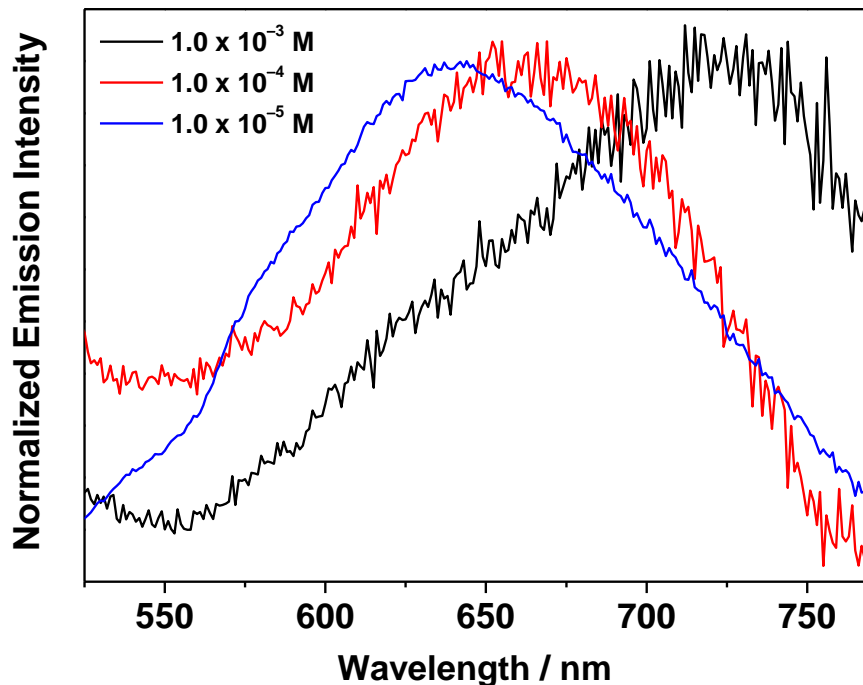


Fig. S9 Normalized emission spectra of **1** in dichloromethane solutions at various concentrations.

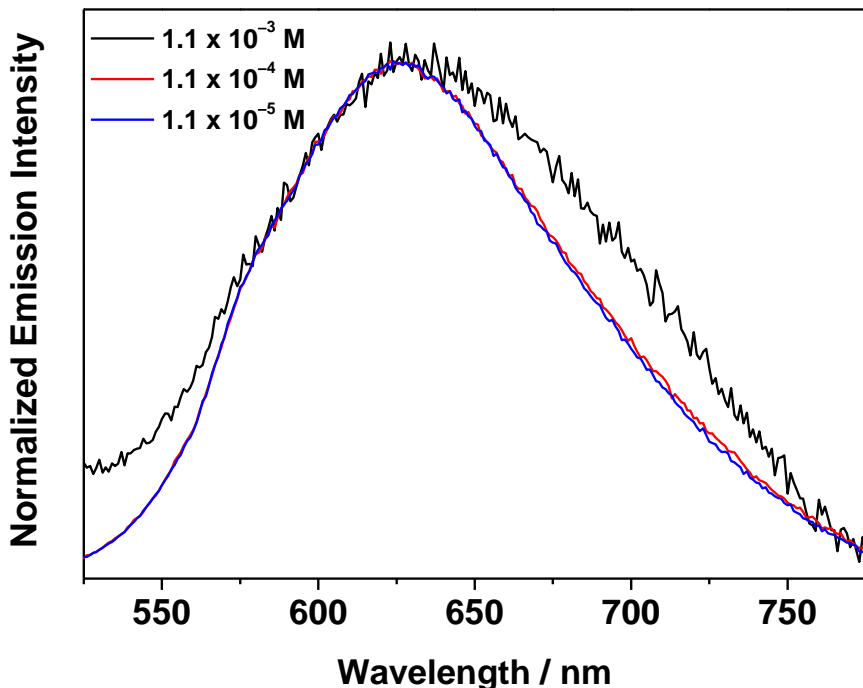


Fig. S10 Normalized emission spectra of **8** in dichloromethane solutions at various concentrations.

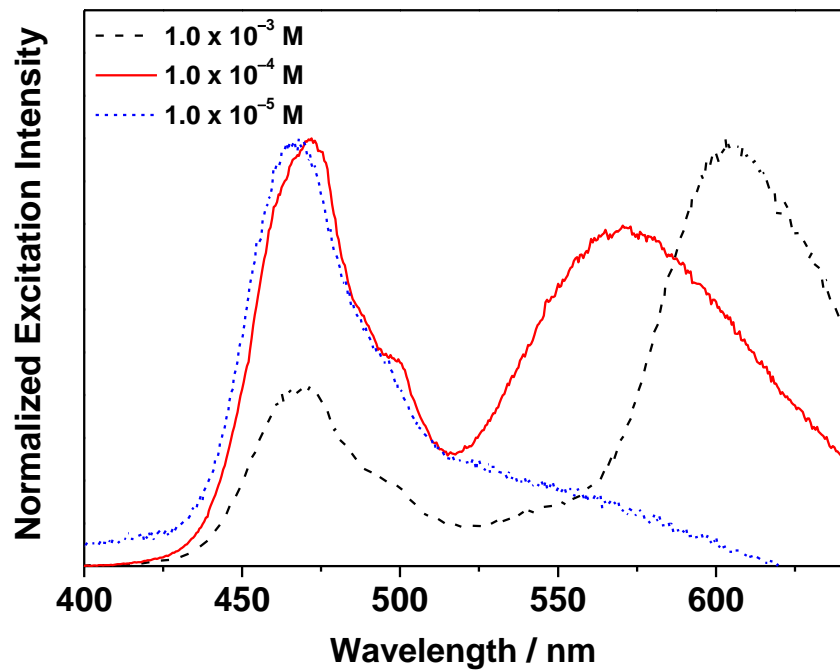


Fig. S11 Normalized excitation spectra of **1** in dichloromethane solutions at concentrations 1.0×10^{-3} , 1.0×10^{-4} and 1.0×10^{-5} M, monitored at 728, 665 and 640 nm respectively.

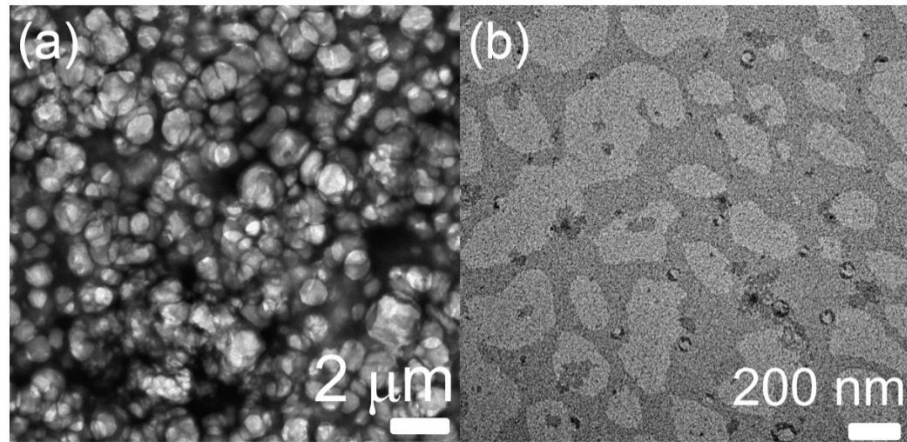


Fig. S12 TEM image of (a) an air-dried sample of a dichloromethane solution of **1** ($[\text{Pt}] = 2.0 \times 10^{-3}$ M) and (b) a sample of a dichloromethane solution of **1** dried under dry nitrogen atmosphere ($[\text{Pt}] = 2.0 \times 10^{-4}$ M).

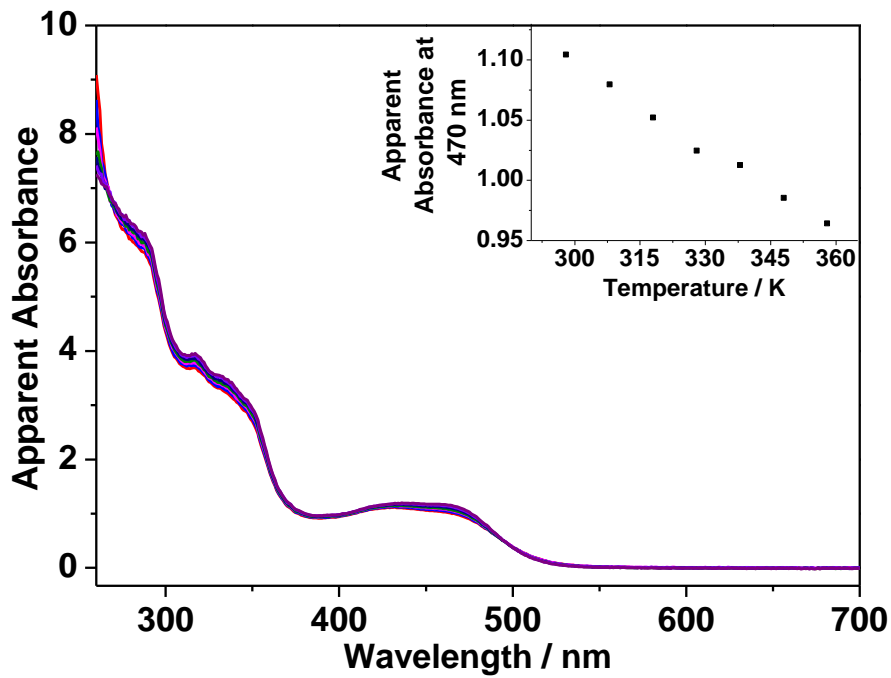


Fig. S13 UV–Vis absorption spectra of **2** in DMSO ($[Pt] = 2.8 \times 10^{-4}$ M) upon decreasing temperature from 358 to 298 K. Inset: A plot of absorbance at 470 nm against temperature. The apparent absorbance values were obtained by correcting to a 1-cm path length equivalence.

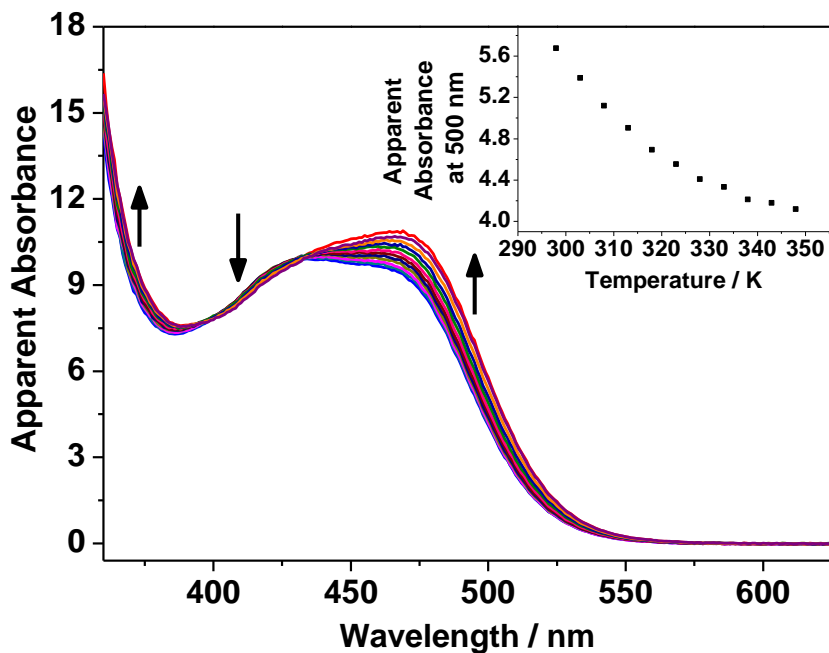


Fig. S14 UV–Vis absorption spectra of **5** in DMSO ($[Pt] = 1.0 \times 10^{-3}$ M) upon decreasing temperature from 348 to 298 K. Inset: A plot of absorbance at 500 nm against temperature. The apparent absorbance values were obtained by correcting to a 1-cm path length equivalence.

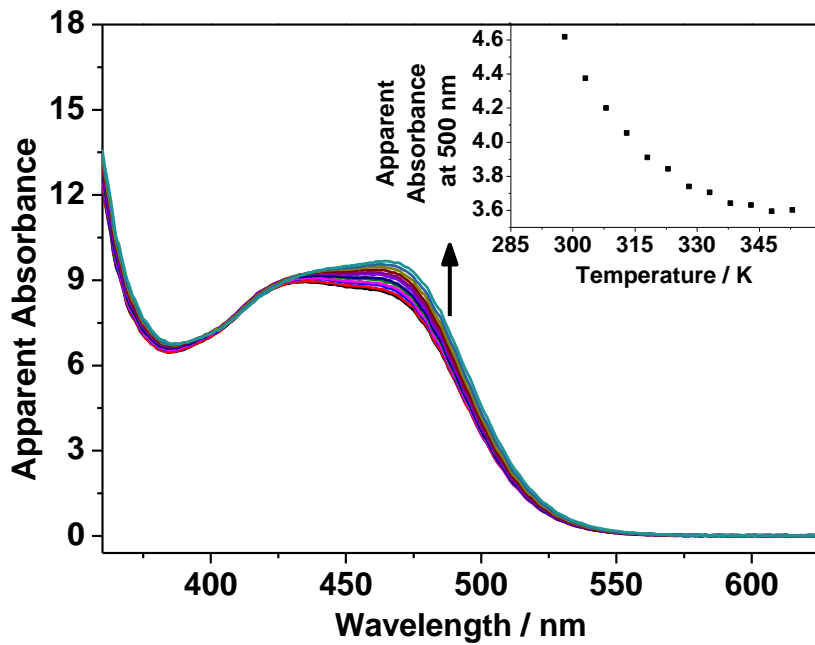


Fig. S15 UV–Vis absorption spectra of **6** in DMSO ($[Pt] = 5.1 \times 10^{-4}$ M) upon decreasing temperature from 353 to 298 K. Inset: A plot of absorbance at 500 nm against temperature. The apparent absorbance values were obtained by correcting to a 1-cm path length equivalence.

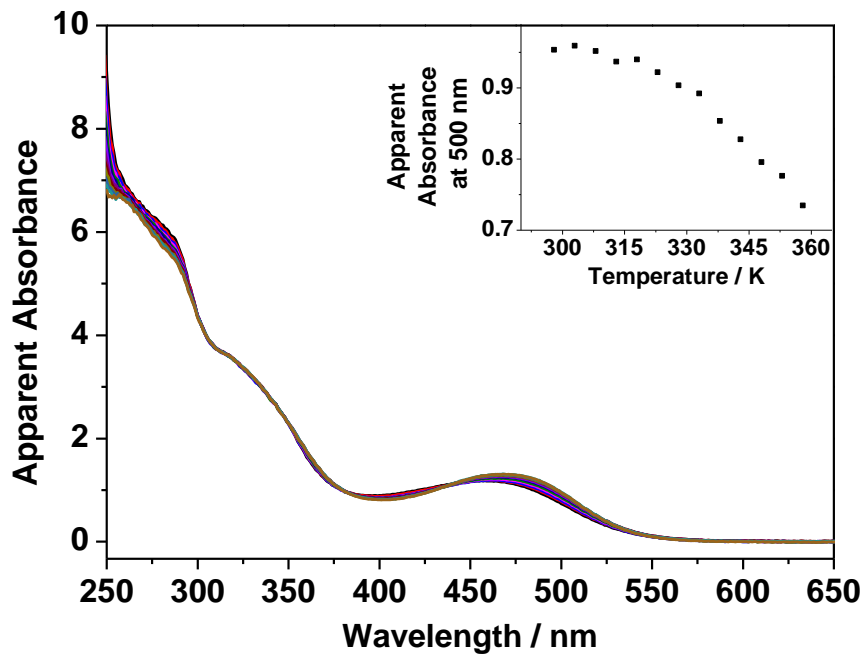


Fig. S16 UV–Vis absorption spectra of **7** in DMSO ($[Pt] = 3.1 \times 10^{-4}$ M) upon decreasing temperature from 358 to 298 K. Inset: A plot of absorbance at 500 nm against temperature. The apparent absorbance values were obtained by correcting to a 1-cm path length equivalence.

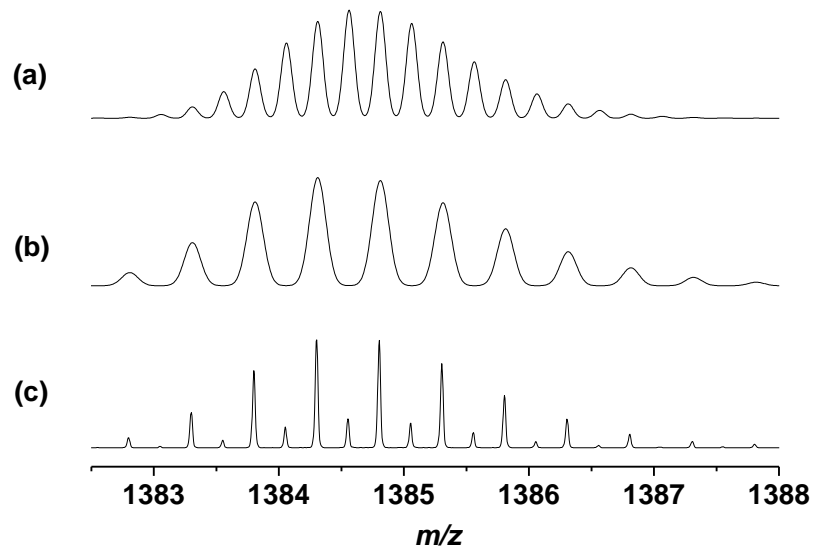


Fig. S17 (a) Simulated dimeric, (b) simulated monomeric and (c) experimental isotope distribution of **4** in its high-resolution ESI mass spectrum.

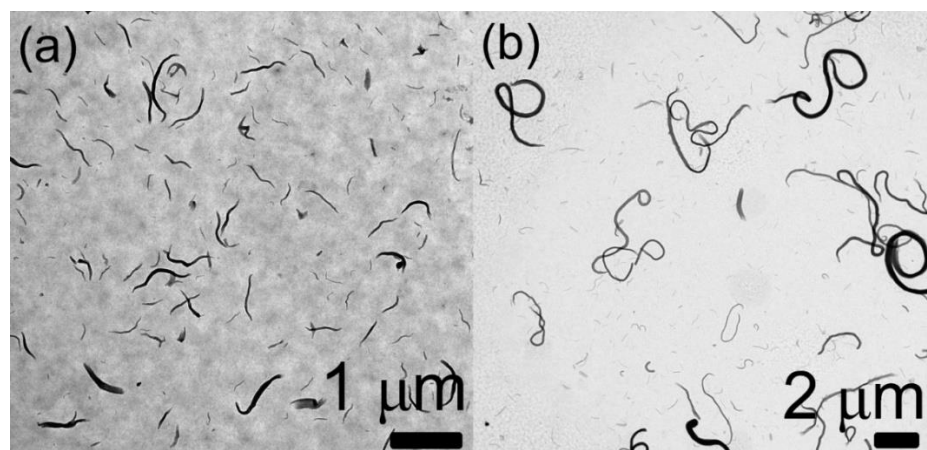


Fig. S18 TEM images of **1** obtained from DMSO solution ($[\text{Pt}]$ = (a) 2.0×10^{-4} M and (b) 2.0×10^{-3} M).

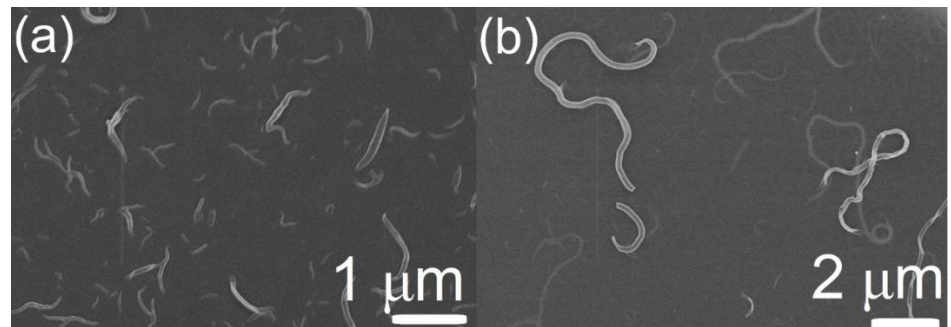


Fig. S19 SEM images of **1** obtained from DMSO solution ($[Pt] =$ (a) 2.0×10^{-4} M and (b) 2.0×10^{-3} M).

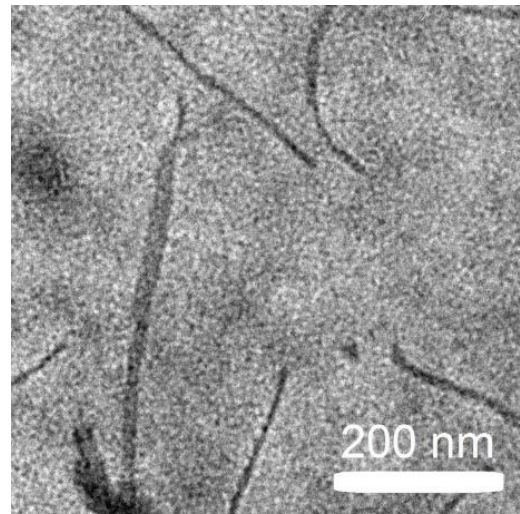


Fig. S20 TEM image of **3** obtained from DMSO solution ($[Pt] = 2.0 \times 10^{-4}$ M).

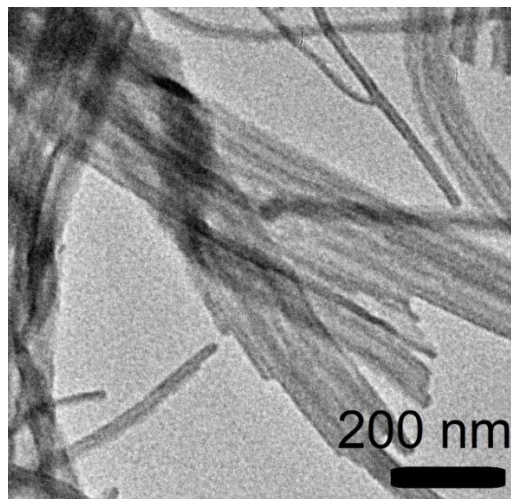


Fig. S21 TEM image of **4** obtained from DMSO solution ($[Pt] = 2.0 \times 10^{-4}$ M).

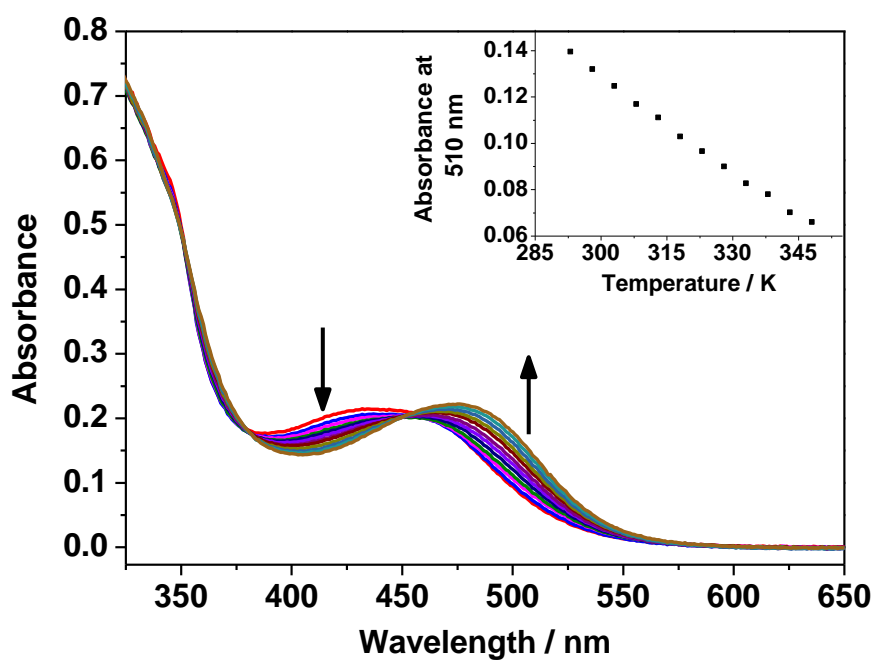


Fig. S22 UV–Vis absorption spectra of **5** in 30 % H₂O in DMSO ($[Pt] = 3.9 \times 10^{-5}$ M) upon decreasing temperature from 348 to 293 K. Inset: A plot of absorbance at 510 nm against temperature.

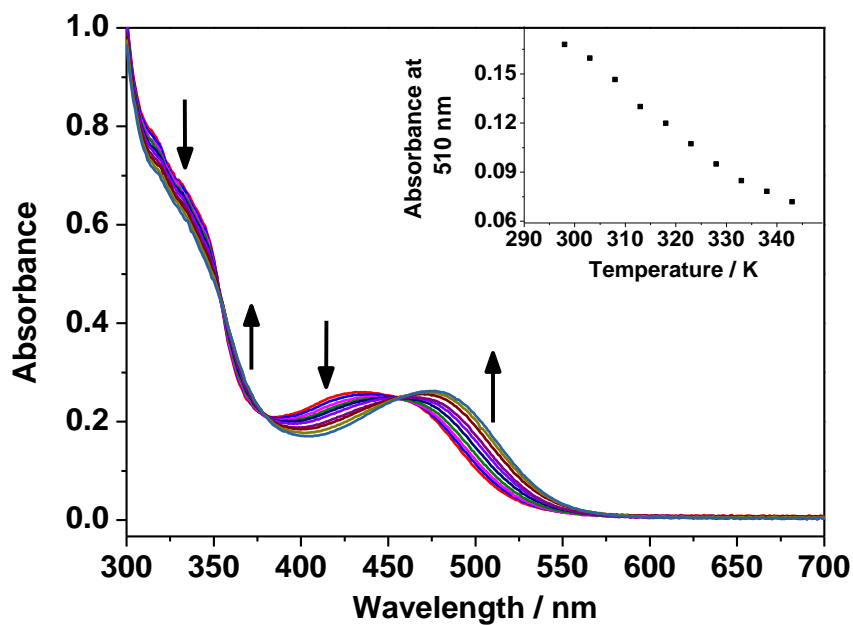


Fig. S23 UV–Vis absorption spectra of **6** in 30 % H₂O in DMSO ([Pt] = 3.5×10^{-5} M) upon decreasing temperature from 343 to 298 K. Inset: A plot of absorbance at 510 nm against temperature.

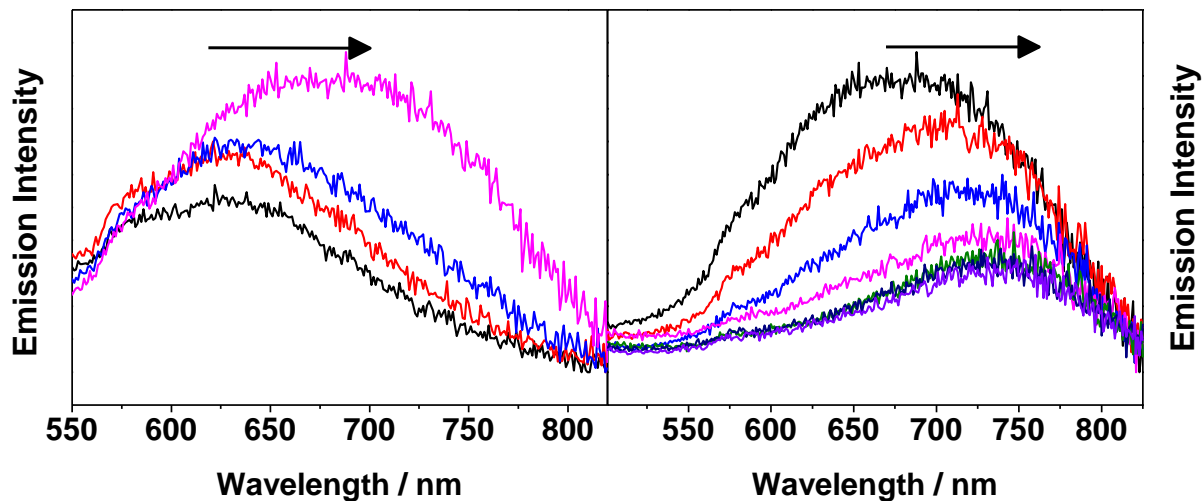


Fig. S24 Corrected emission spectra of **5** upon increasing the water content in DMSO (left) from 0 to 30 % and (right) from 30 to 90 %.

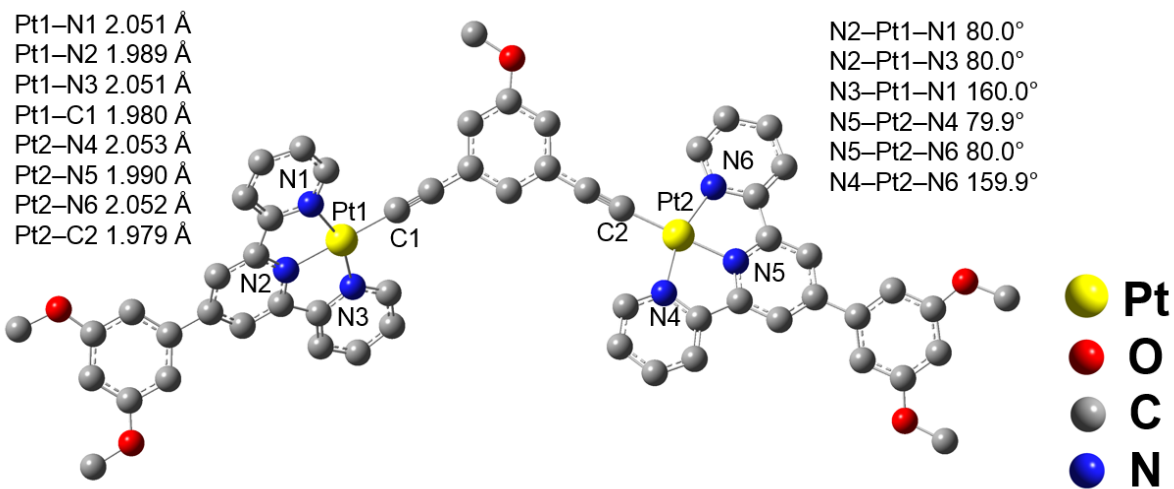


Fig. S25 Selected structural parameters of the optimized ground-state geometries of the model complex of **1**. All hydrogen atoms are omitted for clarity.

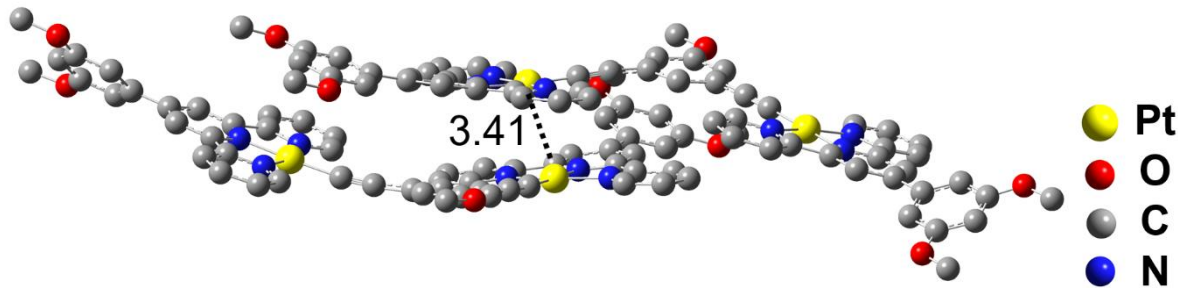


Fig. S26 Optimized ground-state structure of the dimer of the model complex of **1** with head-to-tail stacking. The Pt···Pt distance is in angstroms. All hydrogen atoms are omitted for clarity.

Table S4 Cartesian coordinates of the optimized geometries of the model complex of **1**.

1	C	-7.175705	1.397367	0.577066	58	C	1.16146	-4.378973	-0.232371
2	C	-8.142632	-0.529292	-0.403637	59	H	2.099401	-4.926618	-0.259348
3	C	-9.401687	0.049781	-0.364327	60	O	-0.206071	-6.383379	-0.286628
4	C	-9.547337	1.341413	0.164581	61	C	0.965838	-7.173572	-0.304485
5	C	-8.413482	2.018696	0.640058	62	H	1.573723	-7.014948	0.596441
6	H	-10.266494	-0.478937	-0.755664	63	H	0.636598	-8.21457	-0.330827
7	H	-8.513108	3.009035	1.075696	64	H	1.578543	-6.971158	-1.193258
8	C	-7.777189	-1.864	-0.915871	65	C	2.454749	-2.297312	-0.180103
9	C	-8.691387	-2.757964	-1.448573	66	C	3.542937	-1.728133	-0.171596
10	C	-8.251716	-3.996297	-1.905451	67	Pt	5.31008	-0.836388	-0.143338
11	H	-9.741743	-2.488214	-1.505969	68	N	7.088311	0.054455	-0.106619
12	C	-6.029108	-3.38354	-1.275026	69	N	6.255165	-1.98442	1.269563
13	C	-6.904692	-4.31332	-1.81866	70	N	5.002558	0.632698	-1.541812
14	H	-8.961212	-4.703856	-2.324534	71	C	8.017221	-0.424914	0.735201
15	H	-4.964234	-3.578488	-1.18078	72	C	7.282183	1.109479	-0.91262
16	H	-6.521457	-5.267927	-2.163912	73	C	7.544059	-1.5856	1.514984
17	C	-5.87376	1.922583	1.032308	74	C	5.742358	-3.026143	1.934486
18	C	-5.70825	3.172631	1.606039	75	C	6.100117	1.431787	-1.735232
19	C	-4.439941	3.579132	2.008143	76	C	3.884466	0.85738	-2.241646
20	H	-6.565781	3.825452	1.739857	77	C	9.257074	0.193516	0.794542
21	C	-3.581273	1.483454	1.24461	78	C	8.505976	1.760855	-0.891006
22	C	-3.363277	2.724669	1.826184	79	C	8.320618	-2.25544	2.445827
23	H	-4.301333	4.556661	2.460915	80	C	6.478694	-3.728098	2.878599
24	H	-2.775178	0.774781	1.078309	81	H	4.716167	-3.286762	1.690967
25	H	-2.358376	3.0031	2.126368	82	C	6.062797	2.467998	-2.653448
26	C	-10.877238	1.976767	0.224395	83	C	3.795145	1.885064	-3.170389
27	C	-10.999335	3.354762	0.041483	84	H	3.053453	0.188123	-2.037624
28	C	-12.008586	1.197794	0.471822	85	C	9.512028	1.30327	-0.025994
29	C	-12.259597	3.95099	0.105226	86	H	10.019432	-0.153828	1.486476
30	H	-10.139724	3.980282	-0.186081	87	H	8.694004	2.606329	-1.54676
31	C	-13.263167	1.805567	0.541736	88	C	7.783497	-3.337055	3.136586
32	H	-11.937941	0.127659	0.651292	89	H	9.340606	-1.934517	2.632608
33	C	-13.40067	3.184721	0.360066	90	H	6.022151	-4.56608	3.395027
34	H	-14.37781	3.651483	0.414193	91	C	4.898582	2.698266	-3.379562
35	O	-12.284043	5.284878	-0.097521	92	H	6.940444	3.089728	-2.803704
36	O	-14.297664	0.977822	0.796901	93	H	2.868363	2.032182	-3.715279
37	C	-13.529125	5.953995	-0.027286	94	C	10.820251	1.983433	0.02707

38	H	-14.230551	5.586262	-0.788064	95	H	8.385583	-3.865778	3.869799
39	H	-13.986034	5.852605	0.966207	96	H	4.860865	3.508098	-4.1026
40	H	-13.321441	7.009093	-0.217086	97	C	11.980342	1.243429	0.262056
41	C	-15.594861	1.533279	0.903566	98	C	10.893428	3.365924	-0.151418
42	H	-15.657491	2.258704	1.72572	99	C	13.215292	1.891754	0.308037
43	H	-15.906081	2.017701	-0.031571	100	H	11.958975	0.16194	0.372767
44	H	-16.268999	0.700233	1.113136	101	C	12.132647	4.005333	-0.092164
45	N	-7.090462	0.161258	0.06197	102	H	10.004151	3.973174	-0.302217
46	N	-4.799397	1.088399	0.856949	103	C	13.3031	3.276294	0.136405
47	N	-6.448191	-2.191796	-0.834422	104	O	14.283681	1.095479	0.519859
48	Pt	-5.30191	-0.706347	-0.003446	105	O	12.105874	5.343419	-0.262983
49	C	-3.534775	-1.593979	-0.068666	106	H	14.264296	3.776053	0.178374
50	C	-2.459587	-2.185448	-0.11142	107	C	15.566966	1.689997	0.56673
51	C	-1.231049	-2.913781	-0.156468	108	C	13.326702	6.056775	-0.200554
52	C	-1.256418	-4.31049	-0.2071	109	H	15.816769	2.186781	-0.380276
53	C	0.002779	-2.244792	-0.150449	110	H	15.648114	2.413562	1.388871
54	C	-0.065369	-5.039504	-0.243141	111	H	16.275423	0.877062	0.738871
55	H	-2.202103	-4.848248	-0.213549	112	H	13.808143	5.948451	0.780547
56	C	1.195314	-2.973048	-0.187883	113	H	14.024645	5.734491	-0.984779
57	H	0.031091	-1.1582	-0.114122	114	H	13.07637	7.107787	-0.359343

Table S5 Cartesian coordinates of the optimized geometries of the dimer of the model complex of **1**.

1	C	-3.172011	1.376897	1.188759	115	C	-10.474897	-0.153054	-0.553732
2	C	-2.129369	-0.720047	1.50147	116	C	-11.215271	-2.400604	-0.591462
3	C	-3.359576	-1.338339	1.665395	117	C	-12.495287	-2.013607	-0.222255
4	C	-4.538462	-0.576849	1.583709	118	C	-12.766822	-0.651867	-0.010176
5	C	-4.426973	0.799666	1.315326	119	C	-11.734607	0.285881	-0.175333
6	H	-3.398292	-2.393131	1.903751	120	H	-13.285982	-2.747204	-0.118148
7	H	-5.314703	1.412794	1.240495	121	H	-11.918174	1.336632	0.015931
8	C	-0.788617	-1.325864	1.609032	122	C	-10.708541	-3.764521	-0.836964
9	C	-0.558575	-2.688572	1.723663	123	C	-11.485823	-4.90873	-0.743127
10	C	0.75043	-3.155461	1.798671	124	C	-10.905219	-6.151798	-0.980057
11	H	-1.393892	-3.379541	1.738843	125	H	-12.537219	-4.829277	-0.490211
12	C	1.512153	-0.891544	1.658741	126	C	-8.82262	-5.044499	-1.383674
13	C	1.798839	-2.245631	1.766258	127	C	-9.557447	-6.220082	-1.304516
14	H	0.942755	-4.220329	1.879253	128	H	-11.504842	-7.053316	-0.910697
15	H	2.28345	-0.130804	1.634174	129	H	-7.767332	-5.035456	-1.62826
16	H	2.833264	-2.566796	1.825401	130	H	-9.065682	-7.166906	-1.497151
17	C	-2.837624	2.80825	1.048156	131	C	-9.256068	0.649818	-0.766298
18	C	-3.776495	3.820225	0.909498	132	C	-9.207356	2.030039	-0.640647
19	C	-3.353205	5.143885	0.836848	133	C	-8.005641	2.69454	-0.862973
20	H	-4.832399	3.577795	0.869606	134	H	-10.104015	2.579709	-0.377347
21	C	-1.096763	4.37917	1.042673	135	C	-6.980799	0.578913	-1.316897
22	C	-1.996078	5.427739	0.908166	136	C	-6.878905	1.959646	-1.207132
23	H	-4.081083	5.942055	0.733722	137	H	-7.957896	3.774699	-0.77128
24	H	-0.026416	4.535098	1.106896	138	H	-6.138943	-0.050163	-1.580239
25	H	-1.625026	6.445545	0.865561	139	H	-5.925453	2.441077	-1.393347
26	C	-5.860275	-1.19653	1.824683	140	C	-14.117366	-0.21444	0.392847
27	C	-6.96148	-0.395374	2.147642	141	C	-14.6165	1.008463	-0.060675
28	C	-6.016981	-2.583256	1.744777	142	C	-14.891792	-1.029279	1.221475
29	C	-8.202478	-0.982124	2.392931	143	C	-15.902432	1.407637	0.309557
30	H	-6.884985	0.680291	2.253623	144	H	-14.047889	1.643379	-0.731619
31	C	-7.261245	-3.160059	1.999678	145	C	-16.171841	-0.614151	1.59474
32	H	-5.209553	-3.240329	1.4454	146	H	-14.515663	-1.969175	1.610669
33	C	-8.361553	-2.369578	2.341814	147	C	-16.689198	0.603095	1.140033
34	H	-9.322183	-2.821457	2.548283	148	H	-17.683599	0.917833	1.426692
35	O	-9.211133	-0.126278	2.67107	149	O	-16.311055	2.592144	-0.189582

36	O	-7.324069	-4.503034	1.868812	150	O	-16.84324	-1.455293	2.407657
37	C	-10.470895	-0.673068	3.02193	151	C	-17.627199	3.026527	0.106424
38	H	-10.893745	-1.272331	2.207899	152	H	-18.375427	2.317293	-0.266382
39	H	-10.399551	-1.284664	3.92914	153	H	-17.770188	3.177545	1.182913
40	H	-11.125944	0.177396	3.214227	154	H	-17.750464	3.980585	-0.408136
41	C	-8.539556	-5.150457	2.203332	155	C	-18.151603	-1.093767	2.815295
42	H	-8.799155	-4.986535	3.255911	156	H	-18.15179	-0.156547	3.384104
43	H	-9.368905	-4.816878	1.568699	157	H	-18.828904	-1.002236	1.95801
44	H	-8.368636	-6.214519	2.037347	158	H	-18.498794	-1.902502	3.459747
45	N	-2.080786	0.600999	1.272724	159	N	-10.266615	-1.464144	-0.743321
46	N	-1.501334	3.105151	1.104737	160	N	-8.135246	-0.061179	-1.103327
47	N	0.25605	-0.443117	1.578727	161	N	-9.37818	-3.849512	-1.155074
48	Pt	-0.323368	1.478885	1.332918	162	Pt	-8.451356	-2.055561	-1.209629
49	C	1.420322	2.344602	1.531306	163	C	-6.631398	-2.664017	-1.587118
50	C	2.530903	2.845292	1.683384	164	C	-5.477413	-3.072501	-1.677106
51	C	3.870696	3.326736	1.760012	165	C	-4.114608	-3.489618	-1.658209
52	C	4.14893	4.699941	1.887446	166	C	-3.778744	-4.843895	-1.471376
53	C	4.919925	2.410836	1.639572	167	C	-3.102688	-2.532344	-1.76629
54	C	5.474297	5.138255	1.873383	168	C	-2.436208	-5.217883	-1.394898
55	H	3.326865	5.398621	1.983935	169	H	-4.572669	-5.575796	-1.383987
56	C	6.251044	2.855941	1.602586	170	C	-1.752412	-2.910303	-1.680138
57	H	4.705213	1.352334	1.551187	171	H	-3.360313	-1.488325	-1.90609
58	C	6.521751	4.223125	1.716351	172	C	-1.423904	-4.256239	-1.495699
59	H	7.54193	4.591548	1.690637	173	H	-0.388299	-4.571788	-1.425143
60	O	5.846971	6.42951	1.993531	174	O	-2.014292	-6.488408	-1.214115
61	C	4.826787	7.393664	2.182724	175	C	-2.99892	-7.49882	-1.086792
62	H	4.284556	7.219249	3.120099	176	H	-3.617164	-7.573535	-1.98933
63	H	5.330903	8.359535	2.234879	177	H	-2.455364	-8.434243	-0.947107
64	H	4.119745	7.400028	1.347148	178	H	-3.643937	-7.322299	-0.21768
65	C	7.294044	1.90242	1.412311	179	C	-0.766223	-1.883648	-1.747197
66	C	8.136271	1.031254	1.214933	180	C	-0.057417	-0.88202	-1.77742
67	Pt	9.447084	-0.382063	0.878094	181	Pt	0.852629	0.84882	-1.802221
68	N	10.755178	-1.809148	0.537954	182	N	1.686851	2.626504	-1.807663
69	N	11.093536	0.747193	0.559385	183	N	2.779608	0.311621	-1.517887
70	N	8.242175	-1.995718	1.079379	184	N	-0.786852	1.982947	-2.143476
71	C	12.024689	-1.45503	0.291331	185	C	3.005597	2.705707	-1.58274
72	C	10.332507	-3.08088	0.587287	186	C	0.888627	3.693877	-1.944732
73	C	12.214641	0.007307	0.289101	187	C	3.63829	1.378092	-1.46991
74	C	11.167915	2.082419	0.585473	188	C	3.257837	-0.934602	-1.421022

75	C	8.890686	-3.186095	0.880724	189	C	-0.521152	3.324803	-2.173942
76	C	6.935077	-1.989029	1.363029	190	C	-2.03369	1.542285	-2.340139
77	C	12.974683	-2.441771	0.075146	191	C	3.598451	3.951788	-1.445903
78	C	11.243361	-4.106613	0.38558	192	C	1.434851	4.963615	-1.838114
79	C	13.426921	0.628549	0.034981	193	C	5.004161	1.178604	-1.33449
80	C	12.358336	2.753427	0.339819	194	C	4.615334	-1.187746	-1.27582
81	H	10.244816	2.603749	0.809752	195	H	2.52093	-1.727297	-1.468891
82	C	8.200102	-4.38603	0.952625	196	C	-1.542932	4.239095	-2.389455
83	C	6.198639	-3.162702	1.451425	197	C	-3.087514	2.412672	-2.578146
84	H	6.49291	-1.011718	1.514611	198	H	-2.160555	0.467133	-2.30647
85	C	12.586969	-3.791011	0.123529	199	C	2.806019	5.106406	-1.566401
86	H	14.001691	-2.175644	-0.145158	200	H	4.651283	4.026975	-1.202687
87	H	10.929595	-5.141462	0.451917	201	H	0.811356	5.838777	-1.972091
88	C	13.501687	2.01824	0.059796	202	C	5.500532	-0.118283	-1.239819
89	H	14.30459	0.029849	-0.179942	203	H	5.674282	2.029713	-1.302888
90	H	12.372811	3.836965	0.371608	204	H	4.960547	-2.212874	-1.201329
91	C	6.838274	-4.376473	1.23966	205	C	-2.84028	3.779428	-2.596385
92	H	8.723468	-5.320478	0.78578	206	H	-1.327356	5.301208	-2.404784
93	H	5.14053	-3.111039	1.684625	207	H	-4.078284	2.009433	-2.753924
94	C	13.578361	-4.862398	-0.09607	208	C	3.395475	6.449341	-1.389625
95	H	14.445509	2.515865	-0.137421	209	H	6.568275	-0.281199	-1.13351
96	H	6.290156	-5.310949	1.298761	210	H	-3.643021	4.48705	-2.77512
97	C	14.900182	-4.679455	0.31643	211	C	4.75143	6.658992	-1.648024
98	C	13.191997	-6.052477	-0.71742	212	C	2.596297	7.511161	-0.952899
99	C	15.83582	-5.693958	0.10473	213	C	5.302355	7.930584	-1.475589
100	H	15.217176	-3.778238	0.829996	214	H	5.395364	5.867655	-2.013837
101	C	14.137784	-7.05775	-0.928671	215	C	3.155066	8.780514	-0.792537
102	H	12.180472	-6.207491	-1.07733	216	H	1.54977	7.377471	-0.7028
103	C	15.464307	-6.889011	-0.519555	217	C	4.509791	9.003849	-1.057203
104	O	17.085572	-5.43633	0.541973	218	O	6.617968	8.036972	-1.749308
105	O	13.682443	-8.167107	-1.547017	219	O	2.310147	9.739665	-0.360636
106	H	16.192766	-7.671147	-0.685235	220	H	4.939897	9.988437	-0.931848
107	C	18.078038	-6.430092	0.353295	221	C	7.228233	9.307119	-1.601322
108	C	14.597585	-9.221491	-1.789031	222	C	2.826831	11.044475	-0.160089
109	H	17.827876	-7.354848	0.886788	223	H	6.785799	10.046264	-2.279414
110	H	18.228151	-6.650022	-0.710229	224	H	7.157018	9.669154	-0.568689
111	H	18.999073	-6.016886	0.766553	225	H	8.278825	9.16802	-1.859372
112	H	15.415292	-8.901753	-2.445712	226	H	3.621979	11.048949	0.595163
113	H	15.01266	-9.616191	-0.8542	227	H	3.20618	11.474832	-1.094239

114 H 14.026362 -10.006629 -2.286205 228 H 1.990183 11.646333 0.197186

References

1. G. A. Crosby and J. N. Demas, *J. Phys. Chem.*, 1971, **75**, 991–1024.
2. J. Van Houten and R. J. Watts, *J. Am. Chem. Soc.*, 1976, **98**, 4853–4858.
3. P. Jonkheijm, P. van der Schoot, A. P. H. J. Schenning and E. W. Meijer, *Science*, 2006, **313**, 80–83.
4. P. A. Korevaar, C. Schaefer, T. F. A. de Greef and E. W. Meijer, *J. Am. Chem. Soc.*, 2012, **134**, 13482–13491.
5. G. M. Sheldrick, *Acta Cryst. A*, 2015, **71**, 3–8.
6. M. J. Frisch, G. W. Trucks, H. B. Schlegel, G. E. Scuseria, M. A. Robb, J. R. Cheeseman, G. Scalmani, V. Barone, B. Mennucci, G. A. Petersson, H. Nakatsuji, M. Caricato, X. Li, H. P. Hratchian, A. F. Izmaylov, J. Bloino, G. Zheng, J. L. Sonnenberg, M. Hada, M. Ehara, K. Toyota, R. Fukuda, J. Hasegawa, M. Ishida, T. Nakajima, Y. Honda, O. Kitao, H. Nakai, T. Vreven, J. A. Montgomery, Jr., J. E. Peralta, F. Ogliaro, M. Bearpark, J. J. Heyd, E. Brothers, K. N. Kudin, V. N. Staroverov, T. Keith, R. Kobayashi, J. Normand, K. Raghavachari, A. Rendell, J. C. Burant, S. S. Iyengar, J. Tomasi, M. Cossi, N. Rega, J. M. Millam, M. Klene, J. E. Knox, J. B. Cross, V. Bakken, C. Adamo, J. Jaramillo, R. Gomperts, R. E. Stratmann, O. Yazyev, A. J. Austin, R. Cammi, C. Pomelli, J. W. Ochterski, R. L. Martin, K. Morokuma, V. G. Zakrzewski, G. A. Voth, P. Salvador, J. J. Dannenberg, S. Dapprich, A. D. Daniels, O. Farkas, J. B. Foresman, J. V. Ortiz, J. Cioslowski and D. J. Fox, Gaussian 09 (Revision D.01), Gaussian, Inc., Wallingford, CT, 2013.
7. Y. Zhao and D. G. Truhlar, *Theor. Chem. Acc.*, 2008, **120**, 215–241.
8. Y. Zhao and D. G. Truhlar, *Acc. Chem. Res.*, 2008, **41**, 157–167.
9. A. V. Marenich, C. J. Cramer and D. G. Truhlar, *J. Phys. Chem. B*, 2009, **113**, 6378–6396.

10. D. Andrae, U. Haeussermann, M. Dolg, H. Stoll and H. Preuss, *Theor. Chim. Acta*, 1990, **77**, 123–141.
11. M. Dolg, P. Pyykkoe and N. Runeberg, *Inorg. Chem.*, 1996, **35**, 7450–7451.
12. W. J. Hehre, R. Ditchfield and J. A. Pople, *J. Chem. Phys.*, 1972, **56**, 2257–2261.
13. P. C. Hariharan and J. A. Pople, *Theor. Chim. Acta*, 1973, **28**, 213–222.
14. J. D. Dill and J. A. Pople, *J. Chem. Phys.*, 1975, **62**, 2921–2923.
15. M. M. Frantl, W. J. Pietro, W. J. Hehre, J. S. Binkley, M. S. Gordon, D. J. DeFrees and J. A. Pople, *J. Chem. Phys.*, 1982, **77**, 3654–3665.
16. H.-K. Yip, L.-K. Cheng, K.-K. Cheung and C.-M. Che, *J. Chem. Soc., Dalton Trans.*, 1993, 2933–2938.
17. F. García, M. R. Torres, E. Matesanz and L. Sánchez, *Chem. Commun.*, 2011, **47**, 5016–5018.
18. D. Zhang, D. Li, X. Li and W. Jin, *Dyes Pigm.*, 2018, **152**, 43–48.
19. Y. Morisaki, K. Suzuki, H. Imoto and Y. Chujo, *Macromol. Rapid Commun.*, 2010, **31**, 1719–1724.
20. A. Llanes-Pallas, K. Yoosaf, H. Traboulsi, J. Mohanraj, T. Seldrum, J. Dumont, A. Minoia, R. Lazzaroni, N. Armaroli and D. Bonifazi, *J. Am. Chem. Soc.*, 2011, **133**, 15412–15424.
21. J. Liang, J. Zhang, L. Zhu, A. Duarandin, V. G. Young, N. Geacintov and J. W. Canary, *Inorg. Chem.*, 2009, **48**, 11196–11208.
22. J. G. Rodríguez and T. Laparra, *Tetrahedron*, 2009, **65**, 2551–2555.
23. T. Kaneko, K. Iwamura, R. Nishikawa, M. Teraguchi and T. Aoki, *Polymer*, 2014, **55**, 1097–1102.
24. K. L. Chandra, S. Zhang and C. B. Gorman, *Tetrahedron*, 2007, **63**, 7120–7132.

25. D. Zornik, R. M. Meudtner, T. El Malah, C. M. Thiele and S. Hecht, *Chem. - Eur. J.*, 2011, **17**, 1473–1484.
26. S. Chen, S. Zhang, C. Bao, C. Wang, Q. Lin and L. Zhu, *Chem. Commun.*, 2016, **52**, 13132–13135.